Energy & Environmental Science

ROYAL SOCIETY OF CHEMISTRY

REVIEW

View Article Online
View Journal | View Issue

Cite this: *Energy Environ. Sci.*, 2023, **16**, 830

Nanocellulose-based composite phase change materials for thermal energy storage: status and challenges

Zhenghui Shen,†[a] Mulin Qin,†[a] Feng Xiong,[a] Ruqiang Zou *[abc] and Jin Zhang *[ab]

Thermal energy storage and utilization is gathering intensive attention due to the renewable nature of the energy source, easy operation and economic competency. Among all the research efforts, the preparation of sustainable and advanced phase change materials (PCMs) is the key. Cellulose, the most abundant natural polymer on earth, has the advantages of renewability, biodegradability, recyclability and ease of functionalization, making it a versatile candidate for newly emerging energy applications. Incorporating nanocellulose into PCMs has undergone a booming development as it can overcome the drawbacks of PCMs and form multifunctional sustainable composites. This review summarizes the use of nanocellulose including cellulose nanocrystals and cellulose nanofibers in the field of latent heat storage (LHS). Firstly, the preparation, physical properties and surface modification of nanocellulose are systematically reviewed, followed by the illustration of the preparation of nanocellulose-based materials, including films, hydrogels, foams and aerogels. Then, the fundamentals and applications of PCMs are briefly introduced. In particular, the recent progress in using nanocellulose-based materials for PCM-based LHS applications is intensively reviewed, where nanocellulose-based composite PCM slurries, capsules, fibers, films, and blocks are introduced in detail. The role of nanocellulose in preparing composite PCMs is interpreted from the perspective of its intrinsic properties. Summary and outlook are given to suggest the chances and challenges of using nanocellulose for LHS applications. This work may shed light on the innovative applications of naturally occurring polymers in sustainable energy systems and provide inspiration for the efficient utilization of sustainable thermal energy.

Received 16th December 2022,
Accepted 13th January 2023

DOI: 10.1039/d2ee04063h

rsc.li/ees

Broader context

Expanding the utilization of renewable energy has been considered one effective way to cope with the rising concerns about the ongoing depletion of fossil fuels and the resulting environmental pollution. Thermal energy, a type of clean and renewable energy, can be stored and released through the phase transitions of phase change materials (PCMs). This energy storage and utilization process has the advantages of high energy density, zero carbon emission, low cost, easy operation, recyclability and small temperature swings. Therefore, the preparation of sustainable and advanced PCMs has become the key to green and advanced thermal energy storage applications. Cellulose is the most abundant natural polymer on earth and shows the fascinating merits of biodegradability, renewability, recyclability, environmental friendliness and non-toxicity. Studies on the use of nanocellulose to prepare composite PCMs have emerged in the recent decade; however, there has been a lack of review works. The present review summarizes the state-of-the-art in the preparation and applications of nanocellulose in PCM-based thermal energy storage, as well as the challenges in the further development of nanocellulose-based advanced composite PCMs. We expect that this review will shed light on expanding the utilization of naturally occurring polymers for the preparation of sustainable and advanced composite PCMs for thermal energy applications.

1. Introduction

In the dilemma of ever-increasing environmental concern from society and the constantly growing energy demand, sustainable energy sources such as solar energy, wind energy, and nuclear energy are receiving long-lasting attention from the government, society, industry and academia. The use of thermal

[a] *School of Materials Science and Engineering, Peking University, Beijing 100871, P. R. China. E-mail: rzou@pku.edu.cn, jinzhang@pku.edu.cn*
[b] *Academy for Advanced Interdisciplinary Studies, Peking University, Beijing 100871, P. R. China*
[c] *Institute of Clean Energy, Peking University, Beijing 100871, P. R. China*
† Z. S. and M. Q. contributed equally to this work.

energy storage (TES) technique has been proven to be an effective approach to both reducing energy consumption and addressing the problems related to the intermittency of renewable sources.[1] Specifically, the use of the TES technique offers the advantages of an increase in overall efficiency and better reliability, better economics, reductions in investment and running costs, and less pollution of the environment.[2] Hence, the preparation and utilization of advanced TES systems is of great significance to sustainable and efficient utilization of energy, and consequently helps address the environmental and energy concerns.

TES systems based on latent heat storage (LHS) are the most studied due to their reversible phase transition with fascinating characteristics like high energy storage density and small temperature swings.[3] The function of a LHS system relies on phase change materials (PCMs), which are the media for energy storage and release through their reversible phase transitions. The stored thermal energy can be held for a certain period and released when required, which benefits energy saving and the shift of peak load. PCMs can be categorized into inorganic, organic and eutectic PCMs and each category has its pros and cons. For example, salt hydrates as the representative inorganic PCMs possess the merits of high volumetric energy storage density, non-flammability, non-corrosivity, non-toxicity, and inexpensiveness, which are suitable for both industrial and household applications.[4] However, the phase separation and supercooling issues in their phase transitions need to be overcome for a more efficient TES process. In contrast, organic PCMs such as paraffin and polyethylene glycol suffer little from phase separation and supercooling, but face the challenges of large volume change and the resulting leakage problem.[5] Moreover, thermal conductivity enhancement of PCMs is required for superior energy storage speed and efficiency.[6] For an efficient and reliable TES application, numerous composite PCMs with functional ingredients have been widely developed to cope with the abovementioned weaknesses of PCMs.

Cellulose, a natural polysaccharide consisting of a linear chain of repeating β(1 → 4) linked D-glucose units, is one of the three main components (cellulose, lignin and hemicellulose, as shown in Fig. 1(a)) of green plants and accounts for the most

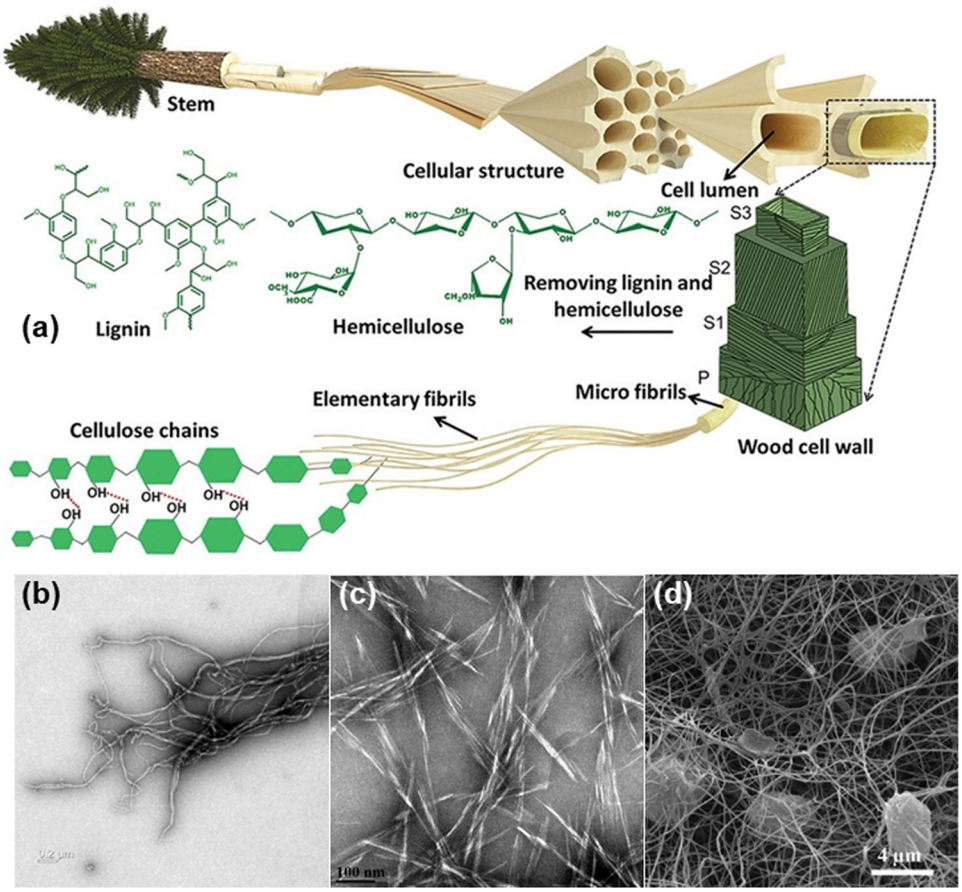

Fig. 1 The hierarchical structure of wood, from the macroscopic level of a trunk to molecular scale of cellulose chains. The wood cell wall has a hierarchical structure composed of the primary wall (P) and the secondary wall (S), which are assembled by cellulose microfibrils with different orientations to the tree growth direction (net-like texture in P, 50°–70° in S1, 5°–15° in S2, and 60–90° in S3); hemicellulose is a non-crystalline and branched polymer that binds with pectin to form microfibrils; and lignin is a 3D amorphous phenolic polymer that probably associates closely with hemicellulose by a lignin–carbohydrate complex through covalent bonds.[23,24] Adapted with permission from ref. 24, Copyright 2021, Wiley-VCH GmbH; TEM image of (b) CNFs produced by a Super Masscolloider grinder, (c) CNCs produced by acid hydrolysis of wood pulp, reproduced from open source under the CC BY license,[25] and (d) bacterial cellulose fibers produced by bacteria *A. aceti*, adapted from open source under the CC BY license.[26]

abundant biopolymers on earth.[7] Cellulose possesses numerous fascinating properties, including biodegradability, renewability, recyclability, environmental friendliness and non-toxicity.[8] Owing to the large amount of hydroxyl groups on its surface, the chemical modification of cellulosic material is of great ease.[9] Nanocellulose, cellulosic material with at least one dimension within the size of 100 nm, has large specific surface area, excellent stiffness, high strength, high aspect ratio and dimensional stability, except for the intrinsic properties of cellulose.[10] Compared to other forms of cellulose-engineered materials, such as cellulose microcrystals and cellulose microfibers, nanocellulose has higher specific surface area and more uniform particle size distribution and thus tends to form a mechanically more stable self-assembled structure. These good properties of nanocellulose meet the requirement of sustainable development and environmental protection, and hence research interest in nanocellulose and nanocellulose-based advanced/functional materials has ever been provoked in recent decades.[11–14] In particular, introducing nanocellulose into PCMs offers the advantages of overcoming the drawbacks of PCMs such as leakage, phase separation, and supercooling for developing advanced and multifunctional composites for sustainable TES systems. With the booming of nanocellulose research, there have been a number of reviews on the application of nanocellulose in energy devices,[15] printed electronics,[16] packing materials,[17] food science,[18] drug delivery,[19] environmental remediation,[20] tissue engineering,[21] *etc.* Although the use of nanocellulose in energy applications has been reviewed,[22] there has been a lack of review on the application of nanocellulose in the latent energy storage field, which will be the focus of this work.

In the present work, a systematic introduction of the preparation, physical properties and surface modification of nanocellulose is given first, followed by an illustration of the preparation of nanocellulose-based materials, including films, hydrogels, foams and aerogels. The basics and fundamentals of TES systems, especially the classification, properties and applications of PCMs, are introduced. Then, an intensive review of the preparation and applications of nanocellulose-based composite PCM slurries, capsules, fibers, films, and blocks is presented. Particularly, the role of cellulose nanofibers and nanocrystals in preparing composite PCMs is compared and interpreted from the perspective of their intrinsic properties. In the end, the challenges of preparing and using nanocellulose-based composite PCMs are summarized.

2. Nanocellulose and nanocellulose-based composite materials

2.1 Preparation and modifications of nanocellulose

2.1.1 Basics of nanocellulose. Nanocellulose is generally categorized into cellulose nanofibers (CNFs), cellulose nanocrystals (CNCs) and bacterial nanocellulose (BC). CNFs and CNCs are typically extracted from natural plant resources like wood, grass and agricultural residues, and BC is usually produced by the biosynthesis process of both Gram negative bacteria like *Gluconacetobacter* and Gram positive bacteria like *Sarcina*.[27] BC usually has a higher crystallinity (over 80%) than that of nanocellulose derived from plant resources (40–85%), greater flexibility, higher hydrophilicity and drug load-release properties, but the disadvantages like time-consuming production, axenic conditions for cultivating specific bacteria and reaction conditions for biosynthesis limit its widespread applications.[28,29] Moreover, the chemical composition and structure of BC are exactly the same as those of CNCs and CNFs; therefore the focus of this article excludes BC. As noticed, CNFs usually have a width of less than 100 nm and a length of several hundreds of nanometers or several micrometers. Compared to CNCs, CNFs are composed of both amorphous and crystalline regions and have higher flexibility.[30] CNCs are rod-like or needle-like, 10–30 nm in diameter and several hundred nanometers in length, and they have high rigidity due to their high crystallinity.[31] Typical electron microscopic images of nanocellulose are presented in Fig. 1(b)–(d).

2.1.2 Preparation and properties of nanocellulose. Cellulose nanofibers are typically "top-down" produced by mechanical processes as shown in Fig. 2(a), such as high-pressure homogenization, microfluidization, and grinding.[32] During the mechanical treatment, cellulosic fiber bundles can be disintegrated by various mechanical impacts, like high pressure, high shear, high speed and turbulence, resulting in aggregated nanofibrils or nanofibril networks. To facilitate the disintegration of cellulose fibers and minimize the intensive energy consumption in the mechanical processes, various pretreatment methods, such as enzymatic hydrolysis, 2,2,6,6-tetramethylpiperidine-1-oxyl radical (TEMPO)-mediated oxidation, carboxymethylation, and quaternization, can be used.[33] The enzymatic pretreatment of cellulose materials usually involves mild conditions and benefits the nanofibrillation of cellulose in the follow-up mechanical processes by creating holes, peeling and fines in the raw materials.[33] The chemical pretreatment could introduce positive or negative charges, reduce the energy input and improve the colloidal dispersion and stability of CNFs.[34] Compared to CNCs, CNFs have different morphological, mechanical and physicochemical characteristics, such as greater length, larger aspect ratios, lower crystallinity, lower modulus and tensile strength, greater flexibility, higher viscosity, and lower gel-forming concentrations. Such property comparison between CNCs and CNFs is available.[35]

Cellulose nanocrystals are usually extracted from lignocellulosic materials using an acid hydrolysis method.[37] In a typical sulfuric acid hydrolysis process (Fig. 2(b)), the amorphous regions of cellulose can be more easily degraded by the strong acid while the crystalline regions are conserved due to their good structure stability. As a result of acid hydrolysis, anionic sulfate groups are inevitably introduced to the surface of CNCs, leading to improved dispersing performance. Although strong acid hydrolysis is a simple and well-developed method to prepare CNCs, more sustainable approaches are required

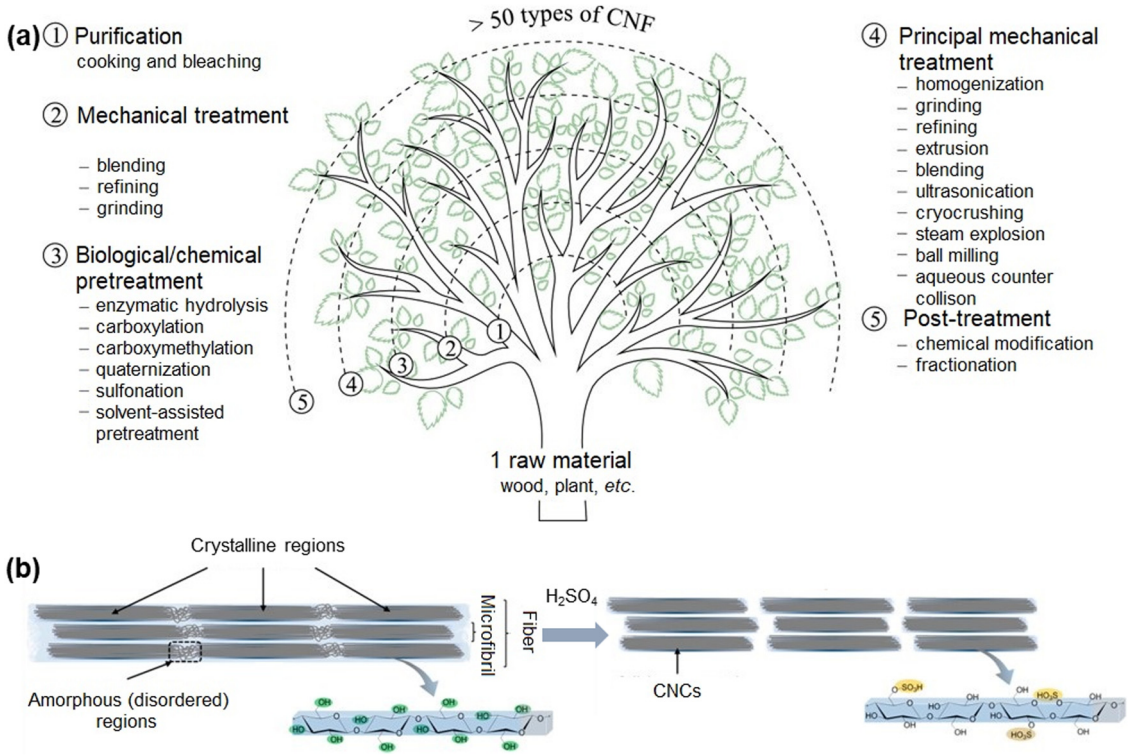

Fig. 2 (a) Summarized methods to produce CNFs, reproduced with permission from ref. 34, Copyright 2016, Elsevier B.V., and (b) schematic diagram of the typical preparation of CNCs by an acid hydrolysis method, adapted with permission from ref. 36, Copyright 2014, American Chemical Society.

owing to the harsh reaction conditions and environmental and safety issues. In recent decades, various solid acids, organic acids, ionic liquids, and deep eutectic solvents have been tested and are shown to be promising alternative ways for obtaining CNCs.[33] CNC crystallinity, ranging from 62% to 90%, is dependent on the starting material for CNC preparation and the crystallinity measurement method.[38] Moreover, the particle morphology, surface chemistry and other characteristics of CNCs are remarkably affected by the material resources and preparation conditions.[38] CNCs exhibit numerous fascinating properties, including high axial stiffness ($\sim$150 GPa), high tensile strength (estimated at 7.5 GPa), low coefficient of thermal expansion ($\sim$1 ppm K^{-1}), thermal stability up to $\sim$300 °C, high aspect ratio (10–100), low density ($\sim$1.6 g cm^{-3}), lyotropic liquid crystalline behavior, and shear-thinning rheology in their suspensions.[39] Motivated by the abovementioned merits of nanocellulose, both CNFs and CNCs have been wildly used in a host of fields, including health, safety, medical, environmental and energy applications in the form of fibers, suspensions, liquid gels, films, aerogels and composites.[39]

2.1.3 Surface modification of nanocellulose. For a better dispersibility, functionability or compatibility with other components or matrices, chemical modification of cellulose is frequently needed. The cellulose surface has abundant hydroxyl groups and these functional groups enable the feasibility of various chemical modifications. Moreover, nanocellulose has a higher degree of surface chemical reactivity due to the nanoscale effect.[10] The chemical modifications of nanocellulose include amination, esterification, oxidation, silylation, carboxymethylation, epoxidation, sulfonation, and thiol- and azido-functionalization and are schematically shown in Fig. 3. Without surface modification, nanocellulose has a strong tendency to aggregate due to the numerous inter- and intramolecular hydrogen bonds derived from the hydroxyl groups. There are typically three classes of nanocellulose surface modifications, including (1) polymer grafting based on the "grafting onto" strategy with different coupling agents (as indicated with blue arrows in Fig. 3), (2) substitution of the hydroxyl group with small molecules (as indicated with red arrows in Fig. 3), and (3) polymer grafting based on the "grafting from" approach with a radical polymerization involving single-electron transfer-living radical polymerization, ring opening polymerization, and atom transfer radical polymerization, as indicated with yellow arrows in Fig. 3.[40] Through nanocellulose modification or functionalization, the nanocellulose–matrix interaction or compatibility can be tuned, and the dispersion state of nanocellulose in the polymer matrix or organic solvents would be improved, leading to favored material processing and fabrication. However, the intensity of hydrogen bonding between nanocellulose and others will be limited with the decrease of the amount of hydroxyl groups on the nanocellulose surface.[41] Besides chemical modifications, physical modification of nanocellulose like plasma treatment, ultrasonic treatment, irradiation, and surface fibrillation[42] and enzymatic modification of nanocellulose *via* direct contact or indirect

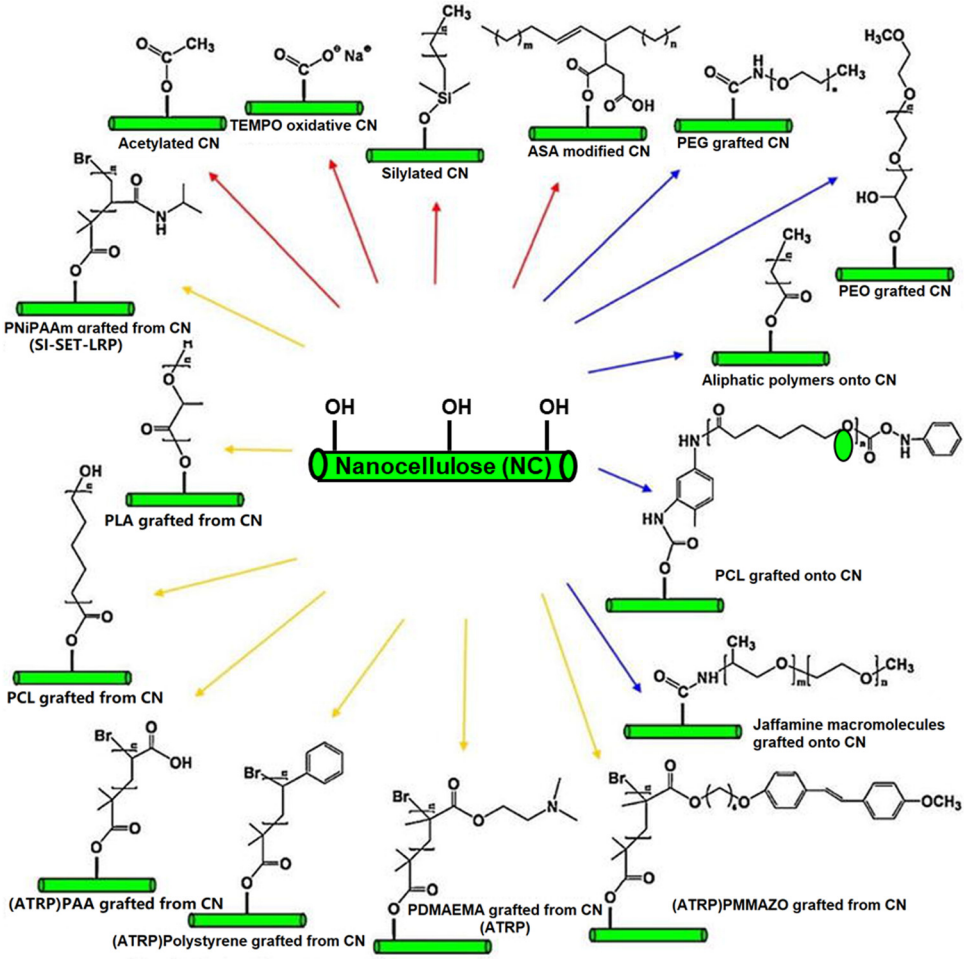

Fig. 3 Schematic illustration of the chemical modifications of nanocellulose. Reproduced with permission from ref. 40, Copyright 2012, Royal Society of Chemistry.

enzyme-mediated modification[43] can be applied. These modifications or functionalizations lead to desired nanocellulose properties, which, in turn, contribute to their effectiveness for the targeted application (*e.g.* food industry[44]) and the satisfactory performance of the final product.

2.2 Nanocellulose-based films

Nanocellulose films can be facilely prepared by either the solvent casting or vacuum filtration method.[45] The obtained nanocellulose films are of fascinating properties, including high surface smoothness, high optical transmittance, excellent flexibility, strong tensile strength, superior gas barrier performance in dry conditions and thermal stability, which help expand their applications from the conventional field such as packing film to newly emerging fields like energy devices, sensors, biomedical and environmental applications.[46]

To endow nanocellulose-based films with functionability, functional additives such as 0D, 1D and 2D nanomaterials can be incorporated.[46] Fig. 4(a) presents the preparation of nanocellulose-based films containing 0D nanomaterials, where aluminum nitride (AIN) nanoparticles were pre-dispersed in the CNF suspension by stirring and ultrasonication, followed by film formation *via* vacuum filtration. The authors studied the effect of AIN dosage on the optical and mechanical properties of the obtained composite films. Their results indicate that without additives, the pristine nanocellulose film exhibits good light transmittance, but upon AIN addition the transmittance decreases and all the composite films become opaque. The optimized CNF–AlN hybrid film has a compact and dense structure with a thickness of 30–40 μm, and its good thermal conductivity, thermal stability and high mechanical strength favor its end use in thermal management of flexible energy storage devices.[47] Besides, metal nanoparticles (NPs), quantum dots (QDs) and others can be incorporated into nanocellulose film structures.[48] 1D nanomaterials, like silver nanowires (NWs), sepiolite (SEP) nanofibers and carbon nanotubes (CNTs), have been successfully used to endow nanocellulose with multifunctionalities, *e.g.* electrical and thermal conductivity and UV blocking performance.[46] In a recent report, Skogberg *et al.* obtained self-assembled CNF/CNT nanocomposite films with anisotropic conductivity through the customized orientation of the high energy sonicated-cationic CNFs (hes-c-CNFs).[49]

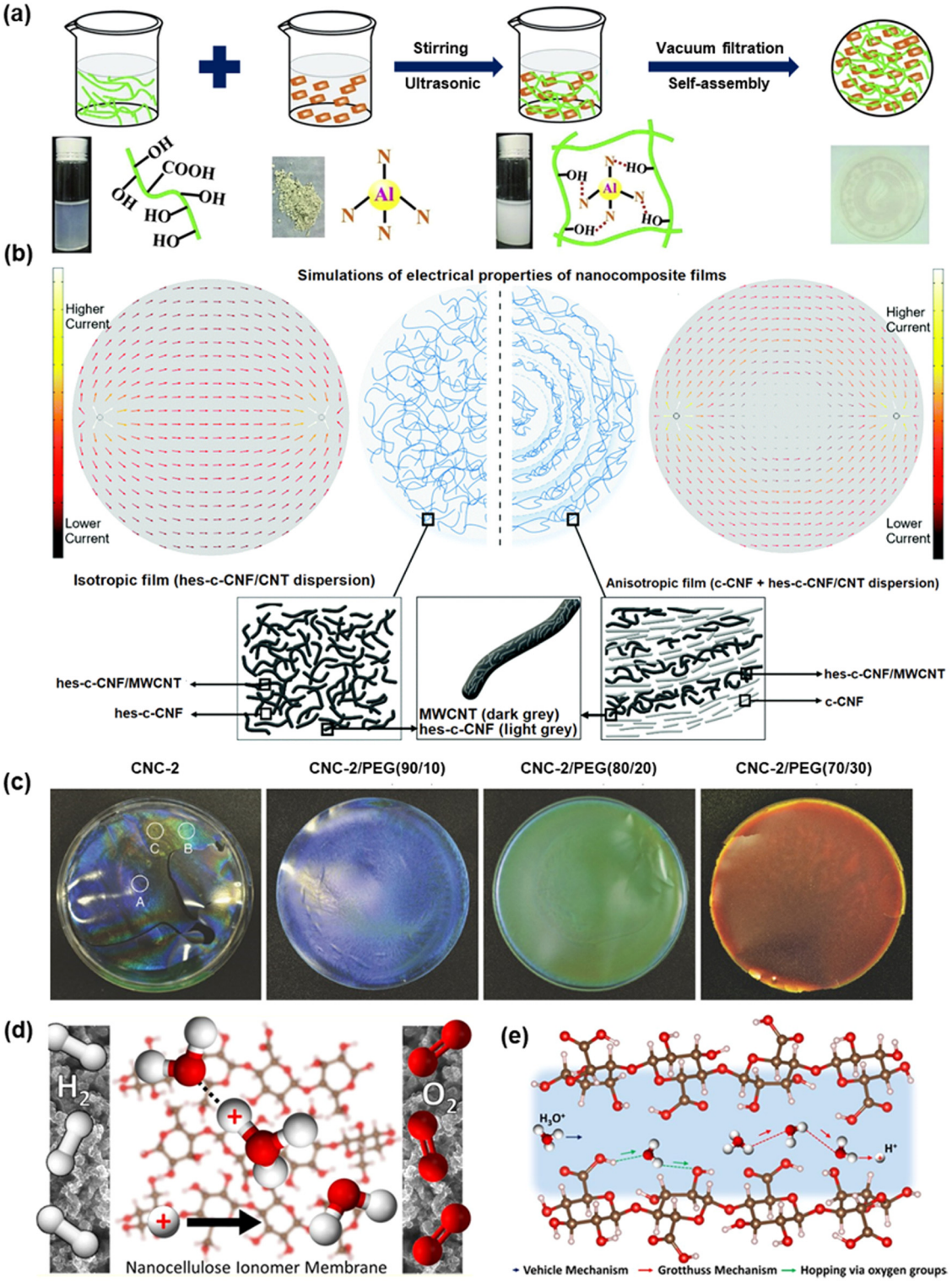

Fig. 4 Preparation and properties of nanocellulose-based composite films. (a) Schematic of the fabrication process of the CNF–aluminum nitride (AlN) nanocomposites, reproduced with permission from ref. 47, Copyright 2019, Elsevier Ltd.; (b) conceptual illustration of the hypothesized structure of nanocellulose/carbon nanotube composite films and their simulated electrical properties: the left side represents the composite film prepared using the hes-c-CNF/MWCNT dispersion and the right side represents the assembled composite film prepared using the c-CNF + hes-c-CNF/MWCNT suspension, adapted under the CC BY-NC license,[49] Copyright 2022, Royal Society of Chemistry; (c) photographs of neat CNC and CNC/PEG composite films showing various structural colors under white light illumination, reproduced with permission from ref. 55, Copyright 2017, Wiley-VCH Verlag GmbH & Co.; (d) schematic of a fuel cell made with a nanocellulose-based ionomer membrane and (e) schematic illustration of the possible proton conduction principle and pathways in nanocellulose, reproduced with permission from ref. 56, Copyright 2016, American Chemical Society.

Fig. 4(b) displays the hypothesized structure of nanocellulose/CNT composite films and their simulated electrical properties, which provides a new solution to prepare nanocellulose-based films with substantial anisotropic conductivity. 2D nanomaterials, such as single or few-layered graphene,[50] montmorillonite,[51] LAPONITE®,[52] and boron nitride,[53] can be combined with nanocellulose to prepare advanced or functional composite films. Intriguingly, nanocellulose has an amphiphilic nature that helps with the dispersion of carbon nanomaterials without deteriorating their intrinsic properties.[54] Nevertheless, when incorporating nanomaterials into the nanocellulose suspension, the ratio between added materials and nanocellulose should be governed for optimal film uniformity and properties.

Polymers can also be applied to prepare fascinating nanocellulose-based films. For example, Jiao *et al.* prepared nanocellulose composite films by introducing copolymer EG-UPy29 and single-walled carbon nanotubes.[57] Through Joule heating, the dynamization and breakage of supramolecular bonds occur at such high temperature, leading to the electricity adaptive softening of the prepared composite films. Moreover, the altered mechanical properties of films are reversibly switchable in power on/power off cycles, suggesting their promising applications in adaptive damping and structural materials, and soft robotics. Zhou *et al.* prepared flexible and responsive CNC-based composite films,[55] and the structural color of the films can be tuned by adjusting the weight ratio between CNCs and polyethylene glycol (PEG) (Fig. 4(c)). In a previous study, the application of a nanocellulose ionomer membrane in fuel cells was reported (Fig. 4(d)),[56] and the proton conduction mechanism of nanocellulose is suggested in Fig. 4(e). Due to the use of nanocellulose, the hydrogen barrier properties of composite films are far superior to those of the conventional ionomer membrane. Moreover, because of the higher conductivity and lower hydrogen gas permeability, fuel cells incorporating CNCs displayed better performance than CNFs due to much lower cell resistance. In addition, the combination of nanocellulose and larger scale cellulose materials such as cellulose microfibers to prepare multiscale nanocellulose composite films has also proved to be a successful material design strategy.[58] Based on this strategy, the strength, toughness and optical properties of the originally brittle nanocellulose membrane could be improved. By introducing multi-scale structural design, nanocellulose composite films can also show an excellent filtration effect and extremely low back pressure, which are hard to be achieved by dense nanocellulose films.[59]

2.3 Nanocellulose-based hydrogels

A hydrogel is usually formed by heterogeneous mixtures of two or more phases, among which the dispersed phase is typically water and the solid phase is a solid three-dimensional network.[31] Because of their low aspect ratio and rigidity, CNCs lack the ability of entanglement, and thus CNCs alone are not suited to be the single component of hydrogels. Instead, CNCs are widely used as reinforcement fillers due to their high mechanical strength. Different from CNCs, CNFs have greater gel-forming capability contributed by their higher aspect ratios and flexible shapes.[60,61]

For a better dispersion of nanocellulose and improved gel uniformity, functional groups or ions are usually introduced. For example, Dong *et al.* fabricated CNF hydrogels with tunable moduli by introducing divalent or trivalent cations (Fig. 5(a)),[62] and it was found that the storage moduli of the gels are considerably dependent on the valency of the metal ions and their binding strength with carboxylate groups on the CNFs. The authors claimed that the driving force for gel formation is the screening of the interfibril repulsive forces originated from the carboxylate charges on the CNF surface, and the strong metal–carboxylate bonding provided a stable screening effect of the repulsive force and contributed to the formation of the CNF gel structure, whose properties are decided by the strength of interfibril interactions and degree of networking. Mendoza *et al.* interpreted the gelation mechanism of nanocellulose gels from the perspective of colloids and interfacial science, and confirmed that elongated nanofiber colloids form cellulosic gels by their entanglement above a critical concentration.[63] As depicted in Fig. 5(b), the stability of the nanocellulose gel network is governed by nanocellulose concentration and the interaction between the surface charges (COO^-), which is dictated by pH and salt. Specifically, decreasing pH and adding salt destabilize nanocellulose gels by releasing bound water, which is ascribed to the decrease in electrostatic repulsion between nanocellulose fibers (Fig. 5(c) and (d)). Lewis *et al.* reported the facile preparation of CNC gels by hydrothermal treatments of their suspensions and the gel properties affected by different factors including temperature, CNC concentration, time and pH (Fig. 5(e)–(h)).[64] Their results indicate that appropriate hydrothermal treatment temperature (below 120 °C), sufficient nanocellulose concentration (higher than 1%), appropriate treatment time (less than 72 h) and pH result in satisfactory gel appearance and stability. Interestingly, pH-responsive nanocellulose gels were prepared by functionalizing CNC surface with either amine or carboxylic acid groups.[65] Under acidic conditions, amine groups are protonated and aqueous dispersions without aggregation are formed due to the electrostatic repulsions of the ammonium moieties and gels form under alkaline conditions because of the hydrogen bonding between CNCs; carboxylic group functionalized CNCs show opposite behavior, *i.e.* nanocellulose is dispersed at alkaline pH and gels form at acidic pH (Fig. 5(i)). The results of shear storage modulus (Fig. 5(j)) indicate that the modulus of amine gels decreases notably when the pH is lowered from 11 to below 9, which agrees with the change in CNC surface charge (*i.e.*, deprotonation of the ammonium ions). In contrast, the modulus of CNCs containing carboxylic groups increased remarkably from 350 Pa at pH 11 to 290 kPa at pH 1, where a gel structure is formed. Hence, it is feasible to tune the gel formation and gel properties by introducing the corresponding functional group or metal ions on nanocellulose surface, and the resulting products are promising for stimuli-responsive applications.

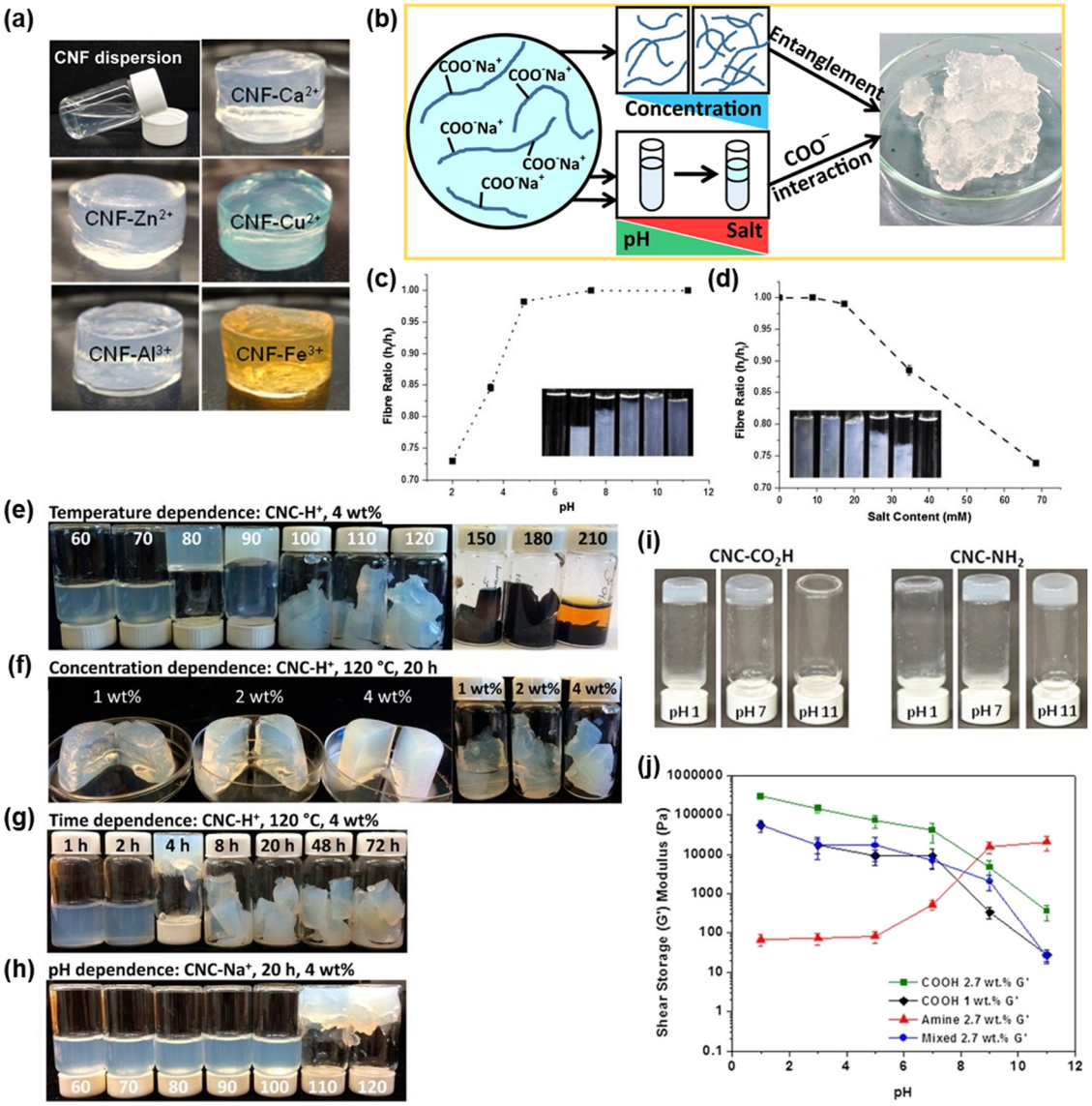

Fig. 5 (a) Digital images of CNF dispersion and free-standing gels formed by addition of metal salt solutions to the carboxylated CNF dispersions, reproduced with permission from ref. 62, Copyright 2013, American Chemical Society; (b) schematic illustration of gelation and colloidal stability of nanocellulose gels driven by entanglement of cellulose nanofibers and electrostatic forces between them, and the effect of (c) pH and (d) salt content on the stability of nanocellulose gels. The fiber ratio is calculated as the ratio between the final height of the gel after centrifugation and the total gel height. The insets show water released from gels under different conditions with pure water as the reference, adapted with permission from ref. 63, Copyright 2017, Elsevier Inc.; digital images of CNC-based hydrogels: (e) hydrogels of 4 wt% CNC–H^+ suspension (pH 2.3) treated at different temperatures for 20 h, (f) hydrogels of CNC–H^+ suspensions treated at 120 °C for 20 h at indicated concentrations, (g) hydrogels of 4 wt% CNC–H^+ suspensions treated at 120 °C for indicated times, (h) hydrogels of 4 wt% CNC–Na^+ suspensions (pH 6.9) treated at indicated temperatures for 20 h, showing the effect of pH on gelation: a higher temperature is required for gelation of CNC suspensions at higher pH; reproduced with permission from ref. 64, Copyright 2016, American Chemical Society; (i) images of aqueous dispersions of 2.7 wt% CNC–CO_2H and 2.7 wt% CNC–NH_2 at pH 1, 7, and 11; and (j) shear storage modulus at different pH of 2.7 wt% CNC–CO_2H, 1 wt% CNC–CO_2H, 2.7 wt% CNC–NH_2, and a mixture of 0.75 wt% CNC–CO_2H and 2.0 wt% CNC–NH_2, reproduced with permission from ref. 65, Copyright 2012, American Chemical Society.

Nanocellulose composite hydrogels with excellent mechanical strength, where CNCs and CNFs serve as reinforcement or fillers, have been intensively reported. Both CNCs and CNFs can be physically or chemically entrapped in the hydrogel networks.[66] The composite hydrogel can be readily prepared *via* simple homogenization and physical entanglement of polymer networks, free radical polymerization of polymeric species within nanocellulose suspensions, UV/ion mediated cross-linking, and cyclic freeze-thaw processes. In the research by McKee *et al.*,[67] the storage modulus of the nanocellulose composite hydrogel increased from 3.8 to 14.3 kPa when increasing the concentration of the CNC from 0.1 to 0.2 wt%, providing stiff and self-healing hydrogel materials for advanced dynamic materials from sustainable sources. Common polymer matrices used for the preparation of CNC-containing gels could be used for preparing CNF-based hydrogels; however, tough yet

highly flexible polymer composite gels can be obtained when using CNFs as reinforcing fillers. Regarding the propensity for entanglement of CNFs, the loading levels of CNFs in the composite gel are typically lower than CNC gels.[66] Yang and coauthors prepared extremely strong and stretchable CNF/PVA nanocomposite hydrogels by suffusing CNF cake with PVA solution followed by room temperature drying and rehydration in water at elevated temperatures (80 °C and 120 °C); the as-prepared composite gel had an elastic modulus of 48 MPa, a fracture strength of 16 MPa, a fracture energy of 2303 J m^{-2}, and a high water content of 67%, showing its promise for human tissue engineering.[68] With the continuous research endeavors, the application of nanocellulose-based hydrogels has expanded to tissue engineering,[69] drug release,[70] wound dressing,[71] sutures,[72] water purification,[73] sensors,[74] supercapacitors,[75] *etc.*

2.4 Nanocellulose-based foams and aerogels

Nanocellulose-based foams and aerogels have been under intensive research due to their low density, high porosity, ease of chemical modification, and more importantly, environmental friendliness. Typically, aerogels refer to nanostructured, porous solid networks with high porosity ($\geq$90%, with a majority of mesopores: 50 nm $\geq$ pore size $\geq$2 nm) and high specific surface area (several hundred square meter per gram);[76] foams refer to solid porous materials with macropores (pore size $\geq$50 nm).[77] Nevertheless, nanocellulosic foams and aerogels are not strictly defined in the literature when describing porous structures or scaffolds based on nanocellulose, and the term ''cellulose aerogel'' is sometimes overused. Despite so, in this article, corresponding terms will be used as they are in the original publications.

The preparation of nanocellulose-based foams and aerogels starts with the preparation of gel, dispersion or wet foam from a cellulose source, followed by the removal of solvent by evaporation (oven drying), freeze drying, and supercritical drying preceded by solvent exchange.[77] As shown in Fig. 6(a), the cellulose sources for preparing cellulosic foams and aerogels also include regenerated cellulose and cellulose derivatives, which, however, are not the focus of this review. Due to the semi-flexible nature of CNFs, cellulose chains easily form entangled networks, and thus CNF-based foams can be directly prepared by removing the solvent from CNF suspension.[78] However, CNC-based foams cannot be facilely prepared in the same way because of the rod-like morphology of CNCs and lack of chain entanglement in CNC dispersion.[79] Preparing porous cellulose structures from wet Pickering foams provides a feasible way to prepare nanocellulose foams and aerogels from either CNFs or CNCs. For example, CNF foam with ultrahigh porosity (99.6%) and low density (6 kg m^{-3}) was prepared by Cervin *et al.* using wet Pickering foams from aqueous dispersions,[80] and the drying of the wet foam was performed in an oven at 60 °C and in a humid environment. It was reported that by adjusting the charge density of the CNF, nanocellulosic foams with different densities could be obtained, and the chemical crosslinking with aldehydes and physical adsorption of octylamine on the CNF successfully tuned the strength and water resistance of the resulting foams, respectively. The effect of wet foaming conditions of a Pickering emulsion on the structural properties of CNF foam was investigated by Park *et al.*,[81] and it was concluded that the consistency of CNF dispersion and the usage of a surfactant affect the wet foam stability and the shrinkage of dry foams, which in turn determine the pore size, porosity and mechanical strength of the dried foam. Qiao *et al.* fabricated ultralight CNC aerogels with hierarchical porous structures from a stabilized Pickering emulsion, where aminated CNCs acted as both stabilizers of Pickering emulsions and building blocks of the nanocellulose aerogels.[82] The resulting aerogels had porosity as high as up to 99.9% and a density of 0.5 kg m^{-3}, which were highly controllable by the composition of emulsion templates and their processing conditions.

Compared to supercritical drying, freeze-drying is widely used to prepare nanocellulose foams due to easy operation and economic reasons. In the freeze-drying process, the generation of a liquid/vapor interface is avoided *via* the ice sublimation principle, and hence other names like lyophilization, cryodesiccation, and ice templating are also used for this drying approach.[84] Before the vacuum-aided freeze-drying, the dispersion or gel is typically frozen to form an ice template, which is then sublimated in a controlled manner to form a porous network. To obtain desired pore distribution and pore morphology, the liquid crystallization, growth of ice crystals and rate of sublimation must be cared for. By creating a temperature gradient inside the starting materials *via* slow cooling, the directional ice templating can be achieved (Fig. 6(b)), and a cellulosic structure having parallel aligned pores can be prepared (Fig. 6(c)). Moreover, bidirectional freeze drying can be performed by tilting the bottom of the container containing nanocellulose-based dispersions to an angle of about 20 degrees, which allows two temperature gradients to be formed along the *Y*-axis and *Z*-axis when contacting liquid nitrogen.[85,86] The fast cooling of starting materials (Fig. 6(d)) by immersing them in ultracold liquid nitrogen (−196 °C) causes water to quickly form ice crystals, leaving dense and tiny pores in the aerogel after sublimation. However, the limitation of this process is the isotropic porous structure (Fig. 6(e)) which prevents the directional mass transfer, heat transfer, and electrical conductivity inside the structure.[87] Ram and coauthors prepared both isotropic and anisotropic piezoelectric CNC aerogels by controlling the ice-templating process.[88] Polyethyleneimine and a crosslinker were used to improve the compressive strength of aerogels. The obtained CNC aerogels exhibited flexibility and high porosity ($>$85%) and satisfactory recovery at 50% compressive strain even after 100 compression–decompression operations. However, the anisotropic CNC aerogels exhibited a greater piezoelectric effect than did the isotropic aerogels, and this can be ascribed to the confinement of CNCs within the aligned porous structure during the directional freezing process. The fascinating mechanical and structural properties of such nanocellulose aerogels favor their applications in sensors,

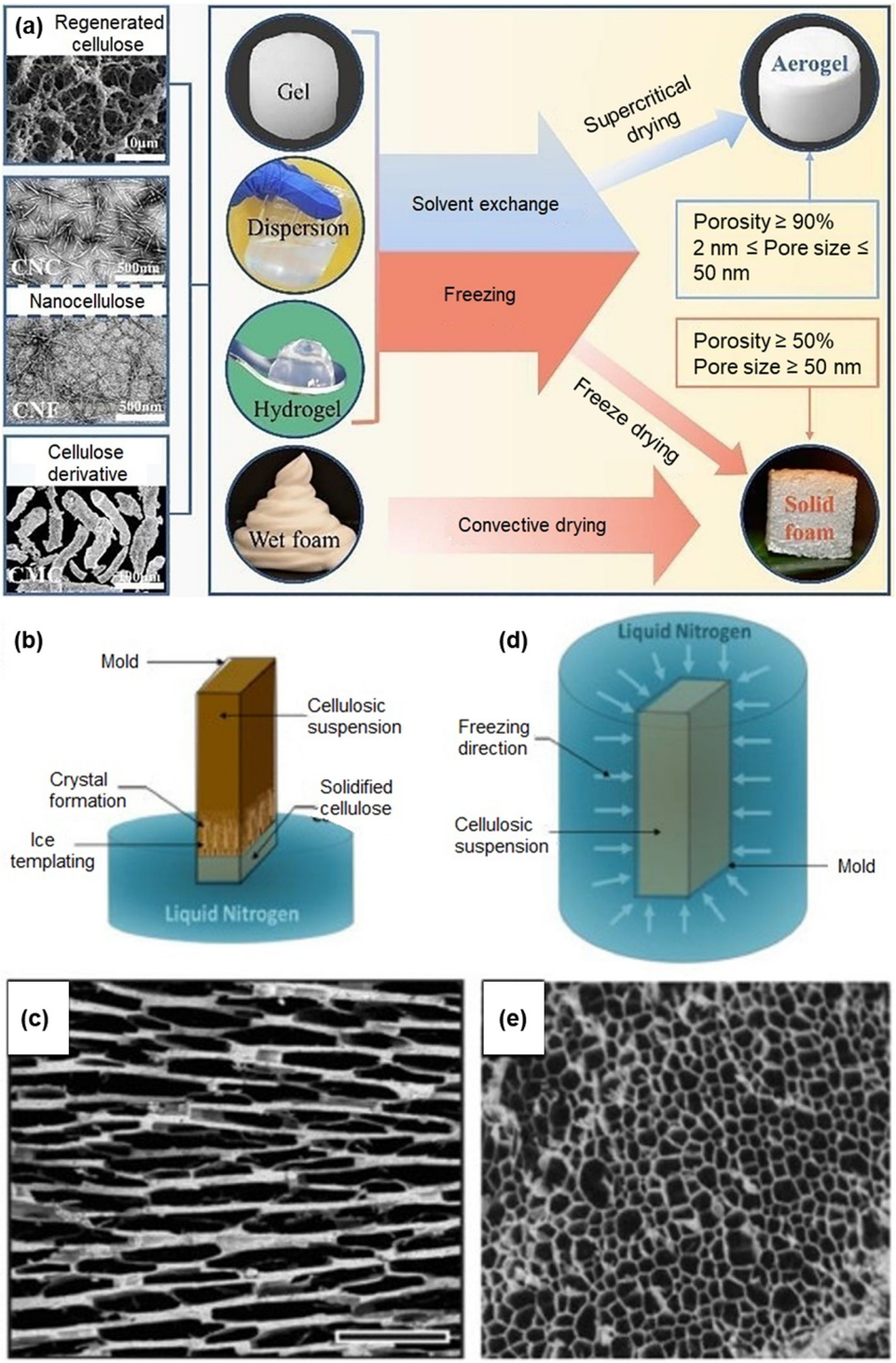

Fig. 6 Preparation of cellulose-based foams and aerogels: (a) fabrication process of cellulose foams and aerogels from regenerated cellulose, nanocellulose and cellulose derivatives, adapted with permission from ref. 83, Copyright 2021, Elsevier B.V.; schematic illustration of the freezing-drying process with variation in cooling processes: (b) slow cooling with directional templating in liquid nitrogen, (c) scanning electron microscope (SEM) image of cellulosic aerogel having parallel aligned pores due to slow cooling, (d) fast cooling with nondirectional templating in liquid nitrogen and (e) cellulosic aerogel with 3D mesopores due to rapid cooling, reproduced from open source under the CC BY-NC-ND license.[84]

wearable sensors, *etc.* Apart from freezing parameters, additives, nanocellulose type and consistency and the drying process have impact on foam structure and properties.[89,90] Through the optimization of these conditions, nanocellulose foams and aerogels with superior structural and mechanical properties and functions can be achieved,

which are promising for advanced applications, *e.g.* wound dressing.[77,91]

3. Latent heat storage and applications

3.1 Overview of thermal energy storage

Thermal energy storage (TES) is a technique that stores or releases thermal energy when heating or cooling an energy storage material so that the stored energy can be used when needed. The stored thermal energy can be used later for many applications, such as space heating, domestic hot water supply, comfort applications in buildings and power generation.[92] Using efficient TES systems, mismatch between power production and demand can be minimized, and the security of energy supply can be guaranteed.[4] Compared to energy systems based on solar energy, wind energy and others, TES systems exhibit higher overall efficiency, competitiveness in investment and running costs, and reduced environmental pollution.[2] Therefore, the research on TES is gathering more attention than ever before.

Typically, TES can be categorized into sensible heat storage (SHS), latent heat storage (LHS) and thermochemical heat storage (THS) based on the technology involved or the energy form.[93] SHS is a simple and well-developed technique, which stores or releases heat relying on the temperature change of the medium. Common materials for SHS include water, brick, concrete, rock, oil and others.[94] Although SHS is the most common and easiest TES form, it shows the intrinsic drawback of low volumetric heat storage capacity,[95] and requires extra facilities (*e.g.* heat pump) to upgrade the temperature level to satisfy the end uses,[96] making it the last option for large-scale energy storage applications. For thermochemical heat storage, energy is stored after a dissociation reaction and then recovered in a chemically reverse reaction. The thermochemical material, used to store thermochemical energy, undergoes either a physical reversible process involving two substances or a reversible chemical reaction. THS systems, although not commercially available yet, have gathered much attention because of their high energy storage capacity and less heat loss.[97,98] Once their drawbacks such as unsuitable operating condition, corrosiveness, environmentally unfriendly production, chemical instability and high cost are overcome, the application of such technology will be boosted.[97]

LHS involves phase transitions of the heat storage materials, heat as a result being stored or released. Due to the engagement of PCMs, LHS exhibits a high energy storage capacity and a small variation in operating temperature among the three TES forms.[99] For a typical solid–liquid LHS process, the temperature continuously increases when being heated, and phase transition occurs as the temperature reaches the melting point of PCMs; the temperature remains steady until the phase transition completes; if being heated continuously, the temperature of the liquid PCM will rise and evaporation or gasification starts. The energy stored in the LHS process consists of sensible heat originated from the heating of PCMs and latent heat originated from the phase transitions of PCMs, and can be calculated by the following equation:

$$Q = m[C_{sp}(T_m - T_i) + \Delta H + C_{lp}(T_f - T_m)] \quad (1)$$

where Q is the total quantity of stored energy by the PCM in the charging process; m is the mass of the PCM; C_{sp} and C_{lp} are the specific heat capacity of the PCM in the solid and liquid state, respectively; T_m is the melting temperature of the PCM; T_i and T_f are the initial and final temperature, respectively; and ΔH is the phase change enthalpy of the PCM.

Various forms of phase transitions exist, including solid–solid, solid–liquid, solid–gas and liquid–gas, and *vice versa*. For the solid–gas and liquid–gas phase transitions, although a large amount of heat is generated, their applications are limited due to the big volume change of PCMs in these processes. Solid–solid PCMs absorb and release heat by reversible phase transitions between a crystalline or semi-crystalline phase, and another amorphous, semi-crystalline, or crystalline phase.[100] Although this process has negligible volume change and thus needs low requirements for PCM containers, such crystal transition usually has low energy storage density and slow transition rate.[101] Solid–liquid PCMs undergo internal molecular arrangement from an ordered crystalline structure (solid) to a disordered amorphous one (liquid) when their temperature reaches the melting point, accompanied by the heat storage process. When the temperature is below the freezing point of liquid PCMs, they recrystallize and form a solid crystalline structure, during which the stored heat is released. Solid–liquid PCMs are predominantly used for energy applications because of their high energy storage density, small volume change and easy handling.[102]

3.2 Phase change materials

Phase change materials that fulfill the energy storage and release processes are the essential component of LHS systems. When selecting PCMs for practical uses, their thermal properties (*i.e.* suitable phase change temperature, high latent heat and good heat transfer), physical properties (high density, small volume change in phase transitions and low vapor pressure), chemical properties (stability, compatibility with surrounding materials, non-toxicity and non-flammability) and kinetic properties (low supercooling and sufficient crystallization rate) should be considered, as well as economic factors (cost-effectiveness and recyclability).[4,103,104] Generally, PCMs can be categorized into solid–solid, solid–liquid, solid–gas, and liquid–gas PCMs according to their phase transitions; they can also be classified as inorganic, organic and eutectic PCMs based on their chemical identity.[94,105,106] For simplicity, an introduction of PCM classification based on their chemistry is given.

Inorganic PCMs include salt hydrates and metallics, among which salt hydrates are typically used because of their high volumetric energy storage density, desirable phase change temperatures, non-flammability, non-toxicity, and inexpensiveness.[107] Salt hydrates with the formula $AB{\cdot}nH_2O$ are crystalline solids that can be considered as the alloys of

inorganic salts and water. In the dehydration (melting) process, salt hydrates break up into an anhydrous salt and free water, or a lower hydrate and water, accompanied by heat storage; in the hydration (freezing) process, the anhydrous salt and water reunite and recrystallize into salt hydrate when system temperature reaches the freezing point, accompanied by heat release. To improve the performance of salt hydrates for TES applications, their intrinsic drawbacks including phase separation, supercooling, relatively low thermal conductivity, and corrosivity must be overcome. Inorganic PCMs also include metallic PCMs, such as low melting metals and metal eutectics. Their advantage lies in the high thermal conductivity, which means that no extra heat exchangers or thermal conductivity enhancers are needed. Besides, metallic PCMs exhibit the merits of thermal stability and reliability, high transition and an impressive working range of temperature (120–1600 °C) that is suitable for special applications like turbine electricity generation.[108] However, metal-based PCMs have not been widely applied for thermal energy storage due to their weight penalties and low latent heat.

Different from inorganic PCMs, organic PCMs usually do not suffer from phase separation and supercooling.[109] Meanwhile, they possess the merits of high latent heat, chemical stability, non-corrosiveness and reusability.[110] Organic PCMs have been intensively used for TES applications, among which paraffin and fatty acids are the representative ones. Paraffin compounds typically comprise straight chain *n*-alkanes (CH_3–$(CH_2)_n$–CH_3), and their melting point and heat of fusion depend on the chain length.[111] Paraffin is one of the most promising organic PCMs for TES applications as it has a high latent heat and excellent thermal properties, including little or no supercooling, a wide range of phase change temperatures, low vapor pressure in the melting process, and good thermal and chemical stability.[112] Nevertheless, paraffin has shortcomings like poor shape-stability, flammability and low thermal conductivity,[94,113] which must be coped with to ensure both the efficiency and safety of TES applications. Fatty acids, among the non-paraffin organic PCMs, show comparable heat of fusion to that of paraffin. Generally, saturated fatty acids rather than unsaturated ones are used in TES, and their phase change temperatures and latent heat increase with the increase of the carbon chain length.[102] Intensively studied fatty acids include caprylic acid, capric acid, lauric acid, myristic acid, palmitic acid, stearic acid, oleic acid, *etc.*[102] Fatty acids are natural PCMs and have the advantages of a promising range of melting temperature, negligible supercooling, congruent melting, lower vapor pressure, suitable thermal and chemical stability, low cost, non-flammability, non-toxicity, and non-corrosivity.[114] Therefore, it is favorable to use fatty acids for TES applications owing to their energy storage performance and environmental and economic concerns.[115] However, like paraffin compounds, they are also weak in form stability and thermal conductivity,[101,116] which limit their widespread applications. Other organic substances like pure alkanes, alcohols, and polyethylene glycol (PEG) also serve as PCMs for LHS applications and their thermophysical properties are summarized elsewhere.[117,118] Besides, the use of ester PCMs has been actively reported,[119–121] suggesting the broad availability of organic PCMs for TES applications.

A eutectic PCM normally consists of two or more components, each of which melts and freezes congruently, forming a mixture of the component crystals during the freezing process.[94] Eutectic PCMs melt and freeze without stratification as the components liquefy or solidify simultaneously during their phase transitions and form uniform mixtures. One advantage of eutectic PCM systems is that their thermal properties, *e.g.* melting point, can be tuned by controlling the ratio between components.[122] The drawbacks of organic eutectic PCMs include low thermal conductivity and leakage during the phase transitions,[123] which limit their energy storage efficiency. Thermal conductive additives or supporting materials can be used to improve the thermal conductivity of eutectic PCMs, and the encapsulation technique and porous scaffolds can be applied to solve the leakage issue. Through the preparation of form-stable composite PCMs with enhanced thermal conduction performance, the use of eutectic PCMs for low- and medium-temperature TES applications such as thermal comfort of buildings could be boosted.[3]

3.3 Composite PCMs for TES applications

Composite PCMs are intensively prepared to overcome the drawbacks of pristine PCMs and to improve their performance, efficiency and reliability for TES systems. In general, composite PCMs with advanced properties are fabricated by incorporating other components, for example, thickening agents for stabilizing salt hydrate PCMs, nucleating agents for decreasing the supercooling degree of salt hydrates, supporting materials for improving the form-stability of organic PCMs, and carbon nanomaterials for enhancing the thermal conductivity of PCMs. These composite PCMs have been utilized in a variety of fields including heat storage and thermal management. The former includes solar energy utilization and industrial waste heat recovery, and the latter includes buildings, batteries, smart textiles, and biomedical applications (Fig. 7).

Heat storage applications. Solar energy as a renewable energy source has attracted great attention due to its convenient availability, inexhaustibility and environmental friendliness. As a solution to efficient utilization of solar energy, PCM systems can be used to convert solar energy to thermal energy and store it for later use, and these systems are derived from the integration of components with high photo-thermal conversion capacity.[125,130] For example, Aftab *et al.* reported that the solar-thermal energy storage efficiency of their developed polyurethane (PU) based composite PCM exceeds 95% when 1% of phosphorene was doped.[131] Other commonly used light absorbing additives include carbon nanomaterials[130] and metallic nanoparticles,[132] which may also enhance the thermal conductivity of PCMs. Besides, in industry productions, waste heat can be generated by diesel engines, industrial processes and thermal power plants. Surprisingly, waste heat accounts for about 16–67% of total energy consumption, and the majority of waste heat can be recovered.[133] Through the efficient recovery

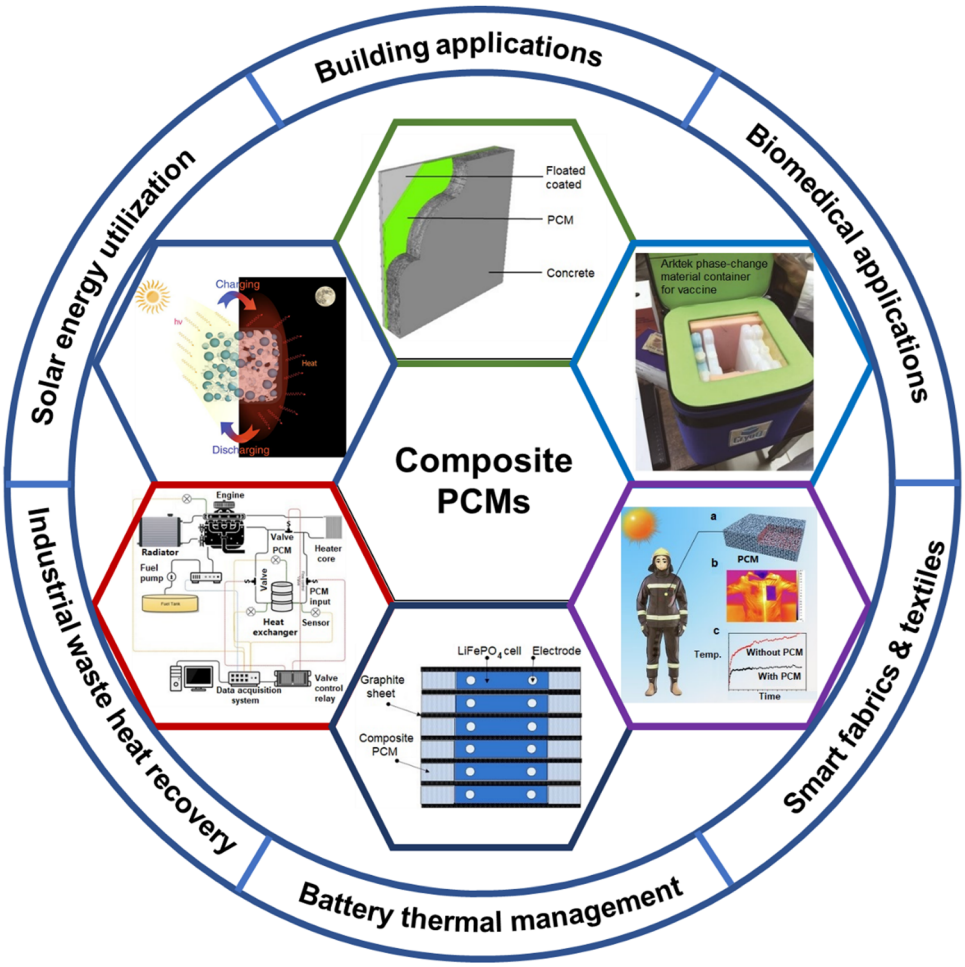

Fig. 7 Schematic illustration of the applications of composite PCMs: application in buildings, adapted with permission from ref. 124, Copyright 2020, Elsevier B.V.; application in solar energy utilization, reproduced from open source under the CC BY license;[125] application in battery thermal management, reproduced with permission from ref. 126, Copyright 2014, Elsevier B.V.; application in industrial waste heat recovery, reproduced with permission from ref. 127, Copyright 2016, Elsevier Ltd.; application in thermos-regulating smart fabrics and textiles, adapted with permission from ref. 128, Copyright 2019, Elsevier B.V.; application in biomedical applications (*e.g.* vaccine storage and transportation), adapted with permission from ref. 129, Copyright 2018, Oxford University Press.

of industrial waste heat, the fuel consumption and pollutant emissions can be reduced and additional economic profits can be obtained if the recovered heat is used for production. The intermittent production of waste heat and its collection remain challenges for its recovery, which can be solved by using PCMs that readily absorb and store heat. The reclaimed latent heat can be extended to terminal utilizations like building heating, hot water supply, and power generation.[134] As mentioned, PCMs exhibit high energy storage density, reversible phase transitions and emit no CO_2. In recent years, a variety of composite PCMs have been developed for such purpose, such as shape-stabilized PEG,[135] stearic acid[127] and paraffin.[136] Through the optimization of PCM-integrated heat storage or recovery systems, a sustainable and economic way for providing energy could be achieved.

Thermal management applications. Buildings consume a lot of energy, among which space heating/cooling and water heating account for approximately 44% for residential buildings and 72% for commercial buildings, respectively.[137] As a response, PCM-based temperature regulation technologies have been developed to reduce the energy consumed in the building sectors. Composite PCMs due to their form-stability and high energy storage density can be used for reducing the heating/cooling load in buildings, where passive heat can be absorbed and released according to the change of environmental temperature. Both inorganic and organic composite PCMs have been reported for building applications,[138–140] and the commonly used scenarios include floors, ceilings, roofs, paints, *etc.* It has been reported that rooms with a composite PCM wall could smartly regulate the indoor temperature while reducing the electricity consumption by over 20% from May to September in Shanghai, China.[138,139] Besides applications for heating/cooling of buildings, supplying household hot water is another popular application. Typically, a PCM-integrated hot water supplying system is integrated with the solar collector and solar water heater.[141] With the great thermal regulation ability

of the PCM, hot water with a constant temperature near the melting point of the PCM is produced and the hot water production time can be adjusted *via* appropriate parameter design of the system. These examples showcase the promising applications of PCMs in shifting the peak load and reducing the heating load of buildings, as well as in developing green and smart buildings.

Battery has become an indispensable energy supplier for human's daily life. During the charging and discharging processes of a battery, lot of heat is produced and the temperature of the battery system increases rapidly, which may cause the thermal runway issue and even cause fire disaster if not properly regulated. Efficient battery thermal management (BTM) is critical to both the safety of end users and the efficiency and lifetime of batteries.[142] Compared to conventional BTM methods like natural cooling, air cooling and liquid cooling, PCMs can absorb a large amount of heat during their phase transitions and maintain the battery temperature at a constant level.[143] As a result, novel BTM systems integrated with PCMs have provoked research interest from academic and industrial communities. For the passive thermal management of the $LiFePO_4$ battery pack, Lin *et al.* developed composite paraffin/expanded graphite sheets,[126] and the results show that PCMs could reduce the temperature rise of the battery during use and improve the temperature uniformity across the battery. To effectively remove the generated heat from the battery, additives with high thermal conductivity could be introduced.[144] However, the flammability of organic PCMs must be addressed when using them for BTM. Owing to their non-flammability and high latent heat, salt hydrate PCMs like $CH_3COONa{\cdot}3H_2O$, $CaCl_2{\cdot}H_2O$ and $Na_2SO_4{\cdot}10H_2O$ have been used for intelligent BTM composites.[145] Meanwhile, the working performance of batteries can be improved in a cold environment by the released heat from PCMs during their phase transitions. Considering the rapid development of battery technologies and the market size, more strategies using PCMs for BTM would emerge in the future; however, the safety, cost and environmental issues should be addressed along with material performance.

Thermo-regulating fabrics and textiles are novel and promising applications of PCMs, where PCMs absorb and store heat through their phase transitions to fulfill the function of temperature regulation and improve the comfort. PCM fibers and yarns as the elemental composition can be fabricated by a host of technologies like electrospinning, centrifugal spinning, melting spinning, solution spinning, dry-jet quenching spinning, interfacial polyelectrolyte complex spinning, vacuum impregnation, and injection spinning, and various polymers such as polyacrylonitrile, polyethylene terephthalate and polyvinyl alcohol can be applied as the supporting material of the resulting PCM fibers. PCM fabrics can be obtained either directly using PCM yarns *via* weaving and knitting, or by modification of the prepared fabric with PCMs in the way of pad–dry–cure coating, grafting, lamination, and printing.[146,147] Composite PCMs with enhanced energy storage performance exhibit a satisfactory thermal buffering effect and are preferred for the fabrication of advanced and functional fabrics and textiles. Salt hydrate–paraffin composite PCMs encapsulated by cellulose foam were fabricated and used for clothing application.[128] The prepared composite PCM has high energy storage density (227.3 J g^{-1}) and flexibility, and it keeps the human body comfortable when exposed to strong sunlight. Advanced and multifunctional composite PCMs are expected to expand their applications in dynamic thermal insulation of textiles such as aerospace, automotive, agriculture, biomedical, defense, sport and casual fabrics and clothing systems, over and above their conventional uses like building construction materials and solar energy storage devices.[112]

The application of PCMs has extended into the biomedical field due to their fascinating thermal regulation properties. The newly emerging applications of PCMs in the biomedical area include cold chains for vaccines and medicines,[129] drug delivery systems,[148] thermotherapy/cold compress therapy and medical dressings.[149] For storage and transportation of vaccines and medicines, a specific temperature range is required; otherwise the vaccines and medicines will be frozen at low temperature and fail at high temperature. The passive cooling carriers with PCMs maintain the required temperature for a long time, making it possible to transport them across a long distance, and this has been reported in the storage and transportation of Ebola Vaccine.[129] For controlled drug delivery or release, PCMs act as the thermo-responsive switch. The encapsulated drug is efficiently released when the temperature is above the melting temperature of the PCM, which can be triggered by direct heating or indirect heating, *e.g.* light irradiation. Therefore, photo-thermal conversion agents, magnetic-thermal conversion agents and acousto-thermal conversion agents, *e.g.* gold nanoparticles and carbon nanoparticles, are typically added.[148] PCM-integrated masks and textiles have also been reported for medical uses,[149–152] showing attractive thermal regulating performances. One thing to mention is that the safety and biocompatibility of PCMs should be considered when using them for certain cases, *e.g.* drug release.

As summarized, the general application area of composite PCMs ranges from energy storage and conversion to advanced medical applications, suggesting their great potential for serving human society. With the ongoing depletion of energy and natural sources, a call on the use of sustainable materials has been proposed. Nanocellulose, as a totally green polymer from nature, exhibits huge potential in preparing advanced and sustainable composites for various fields. The following section systematically reviews the applications of nanocellulose for preparing advanced and sustainable composite PCMs, which may provide inspiration for preparing novel composite PCMs and also for expanding the application of nanocellulose materials.

4. Nanocellulose-based composite PCMs

Compared to synthetic polymers (*e.g.* polymethyl methacrylate, poly(urea-urethane)) and carbon-based materials (*e.g.* graphite,

graphene, carbon nanotubes), nanocellulose has the advantages of natural abundance, renewability, environmental friendliness, safety and low cost. Therefore, it is both economically and environmentally attractive to use nanocellulose for the preparation of composite PCMs. Besides, the capability of forming network in low concentration, the natural amphiphilicity interacting with diverse substances and ease of functionalization of nanocellulose give rise to the possibilities of overcoming the intrinsic drawbacks of PCMs, such as liquid leakage, low thermal conductivity, and supercooling. In recent years, advanced and multifunctional nanocellulose-based PCM composites in the form of slurries, capsules, fibers, films, and blocks have been successfully fabricated for TES applications. This part will intensively review the nanocellulose-based PCM composites and discuss the role of nanocellulose in preparing composite PCMs.

4.1 Nanocellulose-based composite PCM slurries

Nanocellulose has numerous fascinating properties, such as high aspect ratio, large surface area and high strength, as well as the intrinsic merits of cellulose materials like abundant availability, renewability, biodegradability and recyclability. Owing to these good properties, nanocellulose has great potential for preparing novel and advanced composite PCMs. Conventionally, synthetic polymers, such as poly (acrylamide-*co*-acrylic acid) partial sodium salt, sodium polyacrylate, and polyvinyl alcohol, have been applied to address the phase separation issue of salt hydrate PCMs.[153–156] However, the non-sustainability and expensiveness limit their wide applications in energy storage applications. Although carboxyl methyl cellulose (CMC) as a cellulose derivative has been considered as the most prevailing thickening agent for preparing form-stable composite PCM slurries, developing more cost-effective substitutes remains warmly welcomed. Furthermore, the thickening effect of various polymers and additives was simply examined by observing the phase separation behaviors of the PCM slurry, and the mechanism involved needs to be quantitatively explored and interpreted.

CNFs are capable of forming 3D gel-like structures with entangled networks when their concentration is above the critical concentration, and such structures can be obtained at a concentration as low as 0.15 wt%.[60] The network structure provides the frameworks for shape-stable composite PCMs, and the strength of the entangled network can be quantitatively characterized by rheological studies. Besides, the abundant hydroxyl groups on the CNF surface contribute to its compatibility with salt hydrate PCMs. The entangled networks by the compatible nanofibers are expected to provide a stable phase to salt hydrates that are prone to suffer from phase separation in the melting phase transition. Oh *et al.* investigated the effects of different thickening agents on stabilizing sodium sulfate decahydrate (SSD) and the mechanism therein was explored. Cellulose microfibrils (CMFs), unmodified CNFs and TEMPO-oxidized CNFs were selected as the thickening agents, and the phase stability observations (Fig. 8(a)–(d)) suggest that the chemically modified CNF failed to prevent the phase separation of SSD because the nanofibril network structure was destroyed by the high ionic concentration of the dissolved salt. In contrast, CMFs and CNFs successfully avoided the phase separation of SSD as their entangled networks were not damaged by salt dissolution, and CNFs showed a better stabilizing effect due to the higher surface area induced stronger entangling capability than CMFs. The viscoelastic properties of PCM slurries with/without cellulosic thickening agents were measured, and it was confirmed that the pristine CNF exhibited the most promising stabilizing effect for SSD. The phase stability observations verify that the conventional thickener CMC did not function as effectively as CNFs, even when its dosage is higher. The reason was that CMC stabilizes the salt hydrate by increasing the slurry viscosity after its dissolution and there is a lack of entangled network that can prevent the precipitation of the anhydrous salt. This study implies the feasibility of utilizing sustainable nanocellulose to solve the phase separation issue of salt hydrate PCMs.

Inspired by this, entangled network based composite PCM slurries with a stable phase and enhanced thermal conduction performance can be prepared by incorporating nanocellulose and its composites. In recent work, unmodified CNFs were used to enable a stable phase of the sodium acetate trihydrate (SAT) PCM and the optimal CNF dosage and mechanism involved were investigated.[158] When insufficient CNFs were added, phase separation occurred and the slurries could easily flow downward the vials. However, phase stability of the CNFs/SAT PCM slurry was obtained when more than 0.8% of CNFs was added, and the resulting slurry showed weakened fluidity, indicating the effectiveness of using CNFs as a thickening agent. The results of the rheology study of these slurries indicate that the addition of CNFs increased the viscosity (Fig. 8(e)) and storage modulus and yield point (Fig. 8(f)) of slurries, indicating that their solid-like behaviors were enhanced although they all showed shear-thinning flow behaviors (Fig. 8(e)). Moreover, the strength of the entangled CNF network continuously increased up to the CNF addition level of 0.8%, as evidenced by the right shift of the yield point (Fig. 8(f)). The improved viscosity and the physically entangled networks synergistically provide phase stability to the PCM slurry. CNFs/graphene nanoplatelets (GNPs) hybrids were then prepared and added to improve the thermal conductivity of PCM slurries. The amphiphilicity of CNFs can exfoliate and disperse GNPs, but their ratios should be considered for a uniform dispersion. With the addition of CNFs/GNPs hybrids, the resulting PCM slurries exhibited increased viscosity yet the yield point remained unchanged, indicating that the CNFs are the predominant contributor to the phase stability rather than the GNPs. The solidified CNFs/GNPs/SAT composite slurry had a compact structure with decreased pore size, suggesting the compatibility between the components, which can be attributed to the hydrophobic–hydrophobic interactions between CNFs and GNPs and the hydrogen bonding between CNFs and water molecules of the salt hydrate. Fourier transform infrared spectroscopy and X-ray powder diffraction analyses confirmed that these components were physically compounded as all the

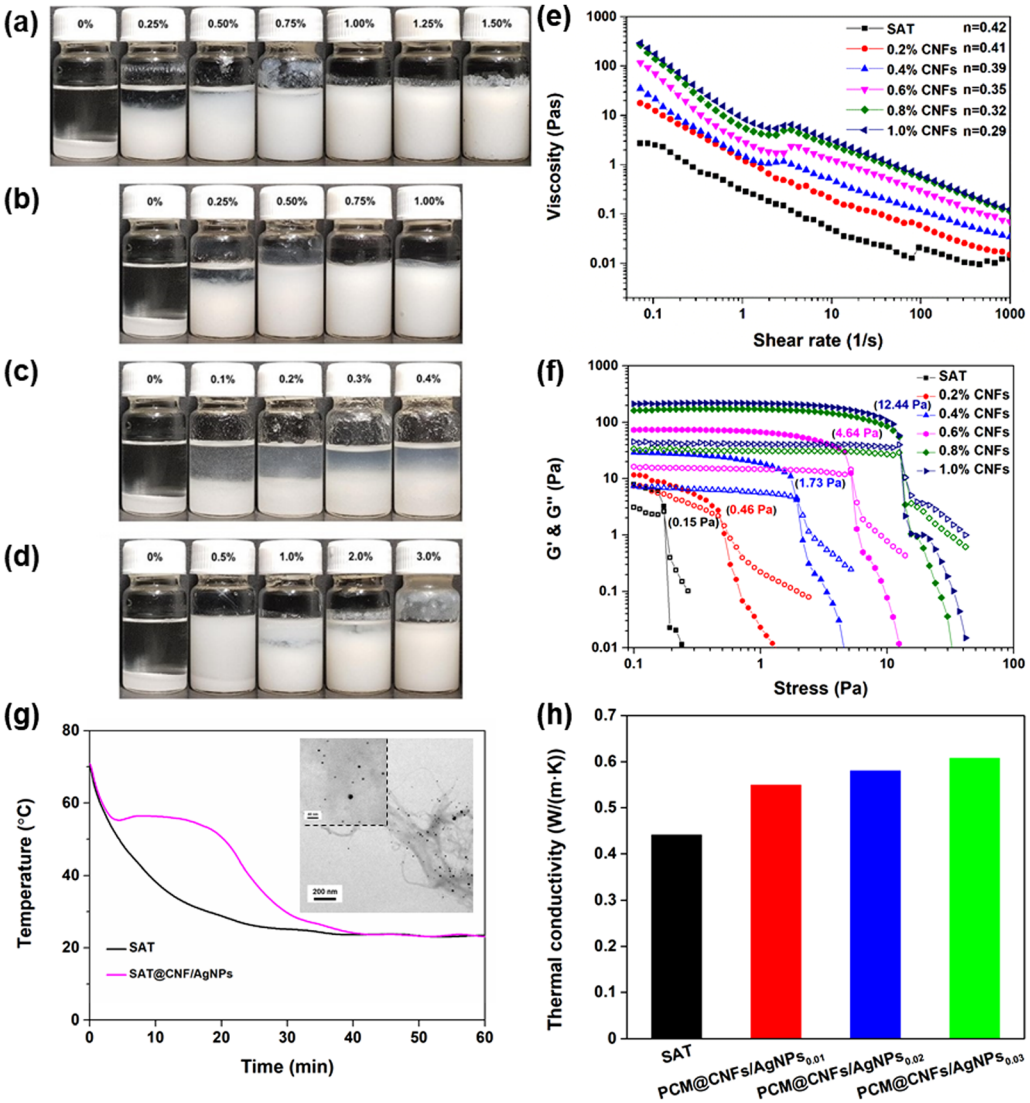

Fig. 8 Phase stability of sodium sulfate decahydrate after 2 h heating in a 40 °C water bath: effect of adding (a) CMFs, (b) CNFs, (c) TEMPO-oxidized CNFs, and (d) CMC, reproduced with permission from ref. 157, Copyright 2020, Springer Nature B.V.; characterization of sodium acetate trihydrate/CNF slurries with varied CNF contents: (e) viscosity as a function of shear rate, (f) amplitude sweep test. Closed symbols in (f): storage modulus (G'); open symbols in (f): loss modulus (G''). Adapted with permission from ref. 158, Copyright 2021, Elsevier B.V.; (g) supercooling degree and (h) thermal conductivity of the composite PCM containing the CNFs/AgNPs hybrid, the inset of (g) presents the transmission electron microscopy image of the CNFs/AgNPs hybrid, adapted with permission from ref. 159, Copyright 2021, Elsevier B.V.

peaks of composite PCMs are simply the mixture of the characteristic peaks of each component without new peaks generated. Moreover, reasonable phase change temperatures and enthalpies and improved thermal stability were found with the addition of CNFs/GNPs hybrids. Owing to the excellent heat transfer performance of GNPs, the thermal conductivity of the composite PCM with 2.5% GNPs improved by 55% over the pure SAT. These improved thermal energy storage performances enable the promising application of SAT for many scenarios, such as household water heating. Likewise, a CNFs/graphite hybrid was used to improve the thermal properties of SSD-based composite PCMs.[160] Absorption of CNFs on the surface of graphite was found, and this indicated their good affinity. Without the addition of CNFs, both SSD and SSD/graphite mixture suffered from the phase separation problem, showing the necessity of using CNFs for a stable phase. When increasing the graphite content in the prepared PCM slurry, the supercooling degree of SSD increased slightly while the melting temperature remained constant. Due to the presence of thermal conduction enhancer graphite and strong interactions between the components, the prepared PCM exhibited improved thermal conductivity and thermal stability, compared with those of pure SSD. As mentioned above, CNFs as a thickening agent are powerful in providing a stable phase to salt hydrates and are capable of dispersing carbon nanomaterials for improving the thermal properties of PCMs.

PCM slurries with greatly suppressed supercooling degree were prepared by the combined use of a salt hydrate and a

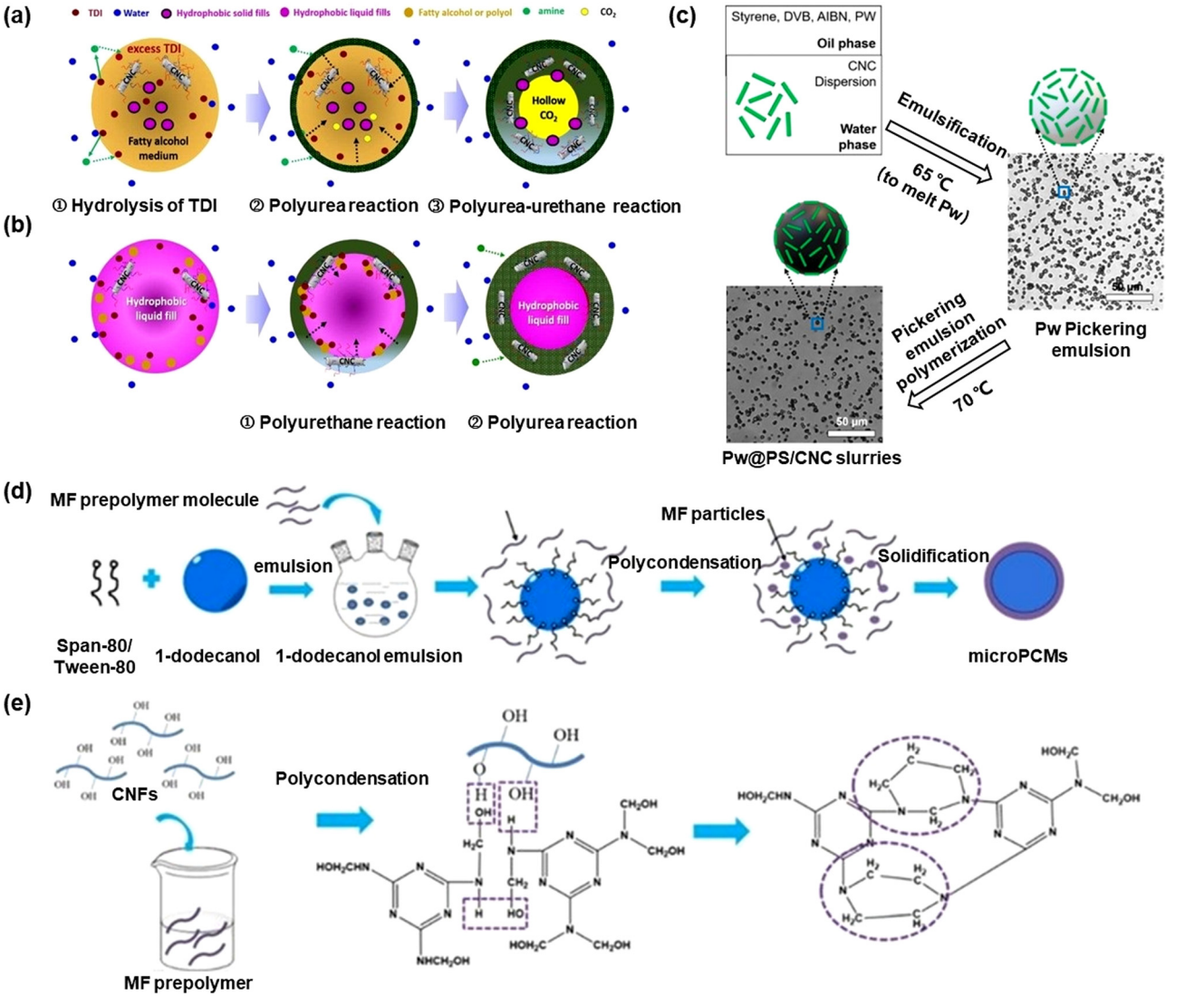

Fig. 9 Encapsulation mechanism of composite PCM microcapsules reinforced by CNCs embedding in the poly(urea–urethane) matrix: (a) hollow capsule and (b) liquid capsule, reproduced with permission from ref. 171, Copyright 2017, American Chemical Society; (c) schematic showing the preparation process of composite PCM microcapsule paraffin wax (Pw)@Polystyrene (PS)/CNC, adapted with permission from ref. 173, Copyright 2019, American Chemical Society; (d) schematic illustrating the preparation process of CNFs/melamine-formaldehyde (MF) composite PCM microcapsules and (e) schematic of the chemical modification of MF by CNFs, reproduced with permission from ref. 174, Copyright 2020, IOP Publishing Ltd.

CNFs/nanoparticles hybrid.[159] Although nanoparticles themselves act as a nucleating agent to decrease the supercooling degree, they are likely to aggregate due to the high surface area and strong van der Waals force. Considering that nanocellulose has been widely used as a stabilizer for nanoparticles,[161] CNF-stabilized silver nanoparticles (AgNPs) were prepared and used to suppress the supercooling of SAT. The CNFs dispersed the synthesized AgNPs uniformly and the silver content of the CNFs/AgNPs hybrid can be facilely tuned by controlling the concentration of the silver ion precursor. The combined use of CNFs/AgNPs and sodium phosphate dibasic dodecahydrate (DSP) showed a synergistic supercooling suppression effect, where DSP worked for the nucleation step of SAT and CNFs/AgNPs facilitated the crystal growth on their surfaces. A minimum supercooling degree of 1.2 °C that is more than 33 °C lower than that of the pure SAT was achieved (Fig. 9(g)). The addition of the CNFs/AgNPs hybrid contributed to a stable phase of the PCM slurry, indicating that the immobilization of AgNPs did not harm the thickening effect of CNFs. Owing to the good compatibility between the components, the prepared composite PCM showed compact structures with uniform distribution of AgNPs, and no chemical reactions occurred among the components. The nanocellulose stabilized metal nanoparticles not only improved the crystallization of the salt hydrate but also enhanced the thermal conduction of the composite PCMs, resulting in an improvement in thermal conductivity by more than 30% (Fig. 9(h)). The phase change temperature and enthalpies changed slightly upon the minor addition of the CNFs/AgNPs hybrid. Moreover, the prepared composite PCMs exhibited enhanced thermal stability over the

pure SAT, and their phase change properties remained almost unchanged after 100 cycles of heating and cooling. In summary, nanocellulose has a great capability of providing phase stability to inorganic salt hydrate PCMs and can stabilize nucleating and thermal boosting nanoparticles. The reported and ongoing research on using nanocellulose to overcome the drawbacks of PCMs and improve their performance for thermal energy conversion and storage sheds light on using naturally occurring and sustainable polymers to fabricate advanced composite PCM slurries.

4.2 Nanocellulose-based PCM capsules

Composite PCM capsules or spheres are usually prepared by encapsulating PCMs with polymers, during which a thin layered shell is formed over PCM droplets. Physical, chemical and physicochemical methods can be used to prepare encapsulated PCMs. Physical methods like centrifugal, spray drying or atomization show the advantages of better economy and easy scale-up, but preparing PCM capsules with a diameter smaller than 100 μm remains a challenge. Interestingly, it is possible to prepare PCM spheres with sizes of 10–20 μm when combining physical and physicochemical methods.[162] Physicochemical methods include the sol–gel technique and coacervation. The sol–gel process comprises the preparation of the metal alkoxide precursor (*i.e.* the sol), followed by the hydrolysis and condensation over the PCM droplets or particles, during which a gel with a three-dimensional network structure is formed.[163] The sol–gel process is capable of preparing PCM microcapsules smaller than 1 μm, and the commonly used shell materials for encapsulation include silicon dioxide and titanium dioxide.[164] Compared to the former two types of methods, chemical methods such as *in situ* polymerization, interfacial polymerization, suspension polymerization, and emulsion polymerization are more prevailing for encapsulation with polymer-based shells, and they are capable of preparing composite PCM spheres with diameter less than 100 μm.[163] Through the encapsulation of PCMs, the PCM leakage issue could be overcome and the reactivity of PCMs with the surroundings could be reduced; the thermal conductivity of PCMs may also be improved if the shell material has relatively high thermal conduction performance. Nanocellulose has been widely used in the fabrication of composite PCMs, where nanocellulose helps either stabilize precursors, or form or strengthen the capsule shell, finally resulting in boosted PCM performances. The prepared nanocellulose-based composite PCM capsules generally have a high PCM encapsulation ratio, reduced leakage and improved mechanical properties, which have been analyzed case by case below.

As a typical protocol, *in situ* polymerization due to its polymeric sealing effect is intensively used for the preparation of shell materials of encapsulated PCMs.[165] Three steps are involved in a typical *in situ* polymerization, *i.e.* formation of oil in water emulsion, formation of capsules, and polymerization of precursors.[166] To prepare the microcapsules with PCM as the oil phase, emulsifiers should be applied to stabilize emulsions in almost all chemical microencapsulation. Compared to the typical synthetic emulsifiers, nanocellulose solid particles are promising stabilizers for microencapsulation or interfaces owing to their excellent sustainability, versatile surface functionalities, safety and low cost.[167] Leakage-free, thermally stable melamine-urea-formaldehyde (MUF)/paraffin microcapsules modified with CNCs by *in situ* polymerization were reported by Han *et al.*[168] In addition to styrene-maleic anhydride (SMA), CNCs produced by the sulfuric acid hydrolysis method were used as co-stabilizers for microencapsulating paraffin, and the effect of adding various amounts of CNCs on the morphology, phase change properties, and size distribution of paraffin/MUF microcapsules was investigated. It was found that the addition of CNCs did not affect the sphere shape of the prepared microcapsules and had no remarkable impact on the crystal type of composite PCMs. However, the thermal stability of microcapsules slightly decreased when increasing the addition level of CNCs. In their later work, the effect of different ratios of CNCs and SMA as stabilizers for microencapsulating PCMs was explored.[169] Although CNCs and SMA both have negative charges, CNCs formed network-like structures in the aqueous phase and increased the viscosity, thereby enhancing the paraffin–water interface stability, even at low SMA concentration.[170] However, without the addition of SMA, almost no PCM capsules were formed as CNCs alone could not stabilize Pickering emulsions for a long time. With the increased portion of CNCs in the mixed emulsifier of CNCs and SMA, the average particle size of the prepared microcapsules increased, and CNCs adhering on the MUF shell were clearly visible. The leakage ratio of the obtained PCM capsules containing 30% CNC stabilizer and 70% SMA stabilizer was as low as 5.37% after a 600 h leakage testing. Their studies show the great potential of using sustainable and versatile CNCs for partially replacing synthetic stabilizers.

The interfacial polymerization method was applied by Yoo *et al.* to prepare poly(urea–urethane)(PU)/CNCs composite microcapsules for controlled dye release.[171] Surface hydrophobization treatments of CNCs by grafting poly(lactic acid) oligomers and fatty acids were conducted to improve the dispersion of CNCs in the polymeric shell. The details of encapsulation are as follows. First, the water-soluble diamine monomer hydrolyzed from tolylene-2,4-diisocyanate (TDI) reacts with the oil-soluble TDI monomer; then, the capsule wall grows toward the oil phase. The fatty alcohol in the oil phase is also consumed by the urethane reaction as an active hydrogen, and then the PU shell grows thicker. The amphiphilic modified CNCs (mCNC) nanoparticles existing mainly at the water/hydrophobic core interfaces are spontaneously embedded into the polymeric shell during the film-forming reaction. Meanwhile, the CO_2 gas (hollow microcapsules, Fig. 9(a)) and hydrophobic ingredients (liquid core microcapsules, Fig. 9(b)) are entrapped in the core. By incorporating mCNCs into the poly(urea–urethane) shell, capsules with strong and dense shells that function as excellent barriers against leakage were obtained. Their study shows the potential of using nanocellulose to make eco-friendly PCM capsules with enhanced shell strength, leakage proof performance and controlled release of specific ingredients. As

follow-up work, microencapsulated methyl laurate PCMs with PU shells containing CNCs were prepared.[172] Same strategies, *i.e.* hydrophobization of CNCs and *in situ* emulsion interfacial polymerization technique, were used to fabricate the nanocomposite shell. Owing to the reinforcement of CNCs that have a high aspect ratio, excellent strength and stiffness, the reported microcapsules have high rupture force and elastic modulus, which is favored for handling or postprocessing like tumbling. Due to the extended diffusion path length by incorporated CNCs, the dense shell structure provides barrier enhancement against the osmotic release of encapsulated PCMs and prevents the PCM leakage issue. Importantly, by tuning the core/shell weight ratios, the encapsulation efficiency and shell thickness of the microcapsules can be facilely controlled. The as-prepared encapsulated PCMs exhibited promising application in building or paving materials owing to their released heat, desired phase transformation temperature, chemical and physical stability, and concrete durability during placement.

Moreover, the Pickering emulsion polymerization technique can be applied for the preparation of encapsulated PCMs. For example, CNCs were used as a Pickering emulsifier and shell component of paraffin PCM microcapsules by Zhang *et al.*[173] As schematically shown in Fig. 9(c), the preparation of composite PCM microcapsule paraffin wax (Pw)@ Polystyrene (PS)/CNC consists of two steps, *i.e.* emulsification of CNC/paraffin melt dispersions by ultrasonication and the Pickering emulsion polymerization process of the styrene shell material at 70 °C for 12 h, followed by a cooling step. It was reported that the prepared PCM microcapsules showed increased latent heat capacity and stability with increasing doses of CNCs owing to the higher surface coverage by these cellulose nanoparticles. The Pw@PS/CNC slurry had a high stability of 99.4% even after 100 heating/cooling thermal cycles. The prepared composite PCM had a paraffin encapsulation ratio of 83.5% that endows it with high latent heat, contributing to its potential as a filling material in isothermal thermoses and hand warmers. In the same work, the authors also used CNC stabilized Pickering emulsions as a template to prepare coconut oil PCM microcapsules, suggesting promising application for buildings because of the moderate melting points of the selected PCM.

A series of microencapsulated PCMs were prepared by encapsulating 1-dodecanol into the CNF modified melamine-formaldehyde (MF) resin *via in situ* polymerization.[174] Fig. 9(d) schematically elucidates the preparation process of composite PCM microcapsules, during which the shell was synthesized by the polycondensation of MF prepolymer molecules, *i.e.* melamine and formaldehyde. Fig. 9(e) shows the preparation of the CNF modified MF resin, which was later used to obtain CNFs/MF encapsulated PCM microspheres. The obtained PCM spheres have a smooth surface and their sizes are 1–3 μm. The cracking ratio testing confirmed that using CNFs greatly improved the rupture resistance of the microcapsules, which could prevent the leakage of PCMs in the preparation and postprocessing steps. The thermoregulation results showed that PCM microcapsules containing CNFs had greater indoor temperature modulation ability over the control, suggesting their promising use in smart building applications. Leakage-proof microencapsulation of PCMs by emulsification with acetylated CNFs was investigated by Shi *et al.*[175] Compared to the pristine CNFs, modified CNFs (mCNFs) provide better compatibility to paraffin PCM and thus improve the encapsulation efficiency and thermal performance. In the microencapsulation process, mCNFs stabilized the transient emulsions with paraffin and then formed a network on the surface of PCM capsules, which functions as a supporting matrix that provides the PCM with shape stability and prevents the leakage issue. Besides, mCNFs act as a nucleating agent that accelerates the heat release process. The prepared composite PCM microcapsules had a high paraffin fraction up to 80% and exhibited an energy absorption capacity of 173 J g^{-1} with their supercooling effectively controlled. These good characteristics indicate the potential applications of these PCM microcapsules for thermal energy conversion and solar energy storage.

Inspired by the fact that CNFs could form a network at oil/water interfaces and prevent the coalescence of oil droplets, Li *et al.* prepared shape-stabilized PCM spheres by encapsulating paraffin PCM with CNFs.[176] In their study, a simple CNF–water–paraffin system was prepared by dispersing paraffin in a 0.2 wt% CNF suspension, followed by ultrasonication treatment to assist in the formation of a stable emulsion. Molecular dynamics simulation was used to study the mechanism of paraffin encapsulation by CNFs, and it was found that the ultrasonication processing allowed paraffin to be dispersed in the water phase in the form of droplets; CNFs in the water phase then diffused to and were stabilized at the paraffin/water interface, leading to the formation of paraffin/CNF core–shell structures. The amphiphilic nature of nanocellulose, where amphiphilicity stems from surfaces or edges with hydroxyl groups and hydrophobicity comes from backbone faces comprising methylene units, contributes to the CNF stabilization effect at the paraffin/water interfaces.[177] Extra CNFs in the system prevented the coalescence of the capsules possibly by forming a network. The formation of a continuous CNF network as the shell not only addressed the leakage issue of this widely used organic PCM but also contributed load-bearing properties to a stimuli-responsive PCM. The resulting composite PCM is lightweight, leakage-free and has a paraffin fraction of more than 72%, displaying the potential to be used for smart building applications.

4.3 Nanocellulose-based composite PCM fibers

To make thermo-regulating textiles and smart garments, composite PCM fibers have been widely investigated. There are several strategies to fabricate thermo-regulating PCM fibers, including immersion of hollow fibers in PCM solutions; composite spinning, in which PCMs are mixed directly with polymer melts or solutions for spinning, and the resulting fibers have shell–core or ''sea-island'' structures; and microcapsule spinning, in which microcapsules containing PCMs are mixed with polymer melts or solutions for spinning.[178] A number of composite PCM fibers have been fabricated by these methods. For example, thermally sensitive PCM fibers were prepared by

immersing hollow rayon and polypropylene fibers into aqueous solutions of calcium chloride hexahydrate/strontium chloride hexahydrate.[179] PCM nanofibrous composites for thermal energy management were obtained by the electrospinning of homogeneous solutions that contain polyethylene glycol, polyvinyl alcohol PCMs and $AgNO_3$ and TiO_2 nanoparticles.[180] Paraffin/polymer composite nanofibers for thermal comfort applications were fabricated by a two-step process, in which the PCM nanocapsules were prepared by emulsion polymerization followed by the electrospinning of polyacrylonitrile/PCM nanocapsules.[181] In particular, electrospinning is a simple, convenient, and versatile technique for fabricating ultrafine composite fibers from a wide variety of polymers, polymer blends, and nanoparticle-impregnated polymers,[182] and is serving a critical role in fabricating composite phase change fibers.

For preparing composite PCM fibers, nanocellulose can be used either as a functional filler of phase change fibers or as a supporting matrix of PCMs, and importantly, it is green, economic and safe. Furthermore, cellulose derivatives, especially cellulose esters, are welcomed for the preparation of composite PCM fibers. By using cellulose derivatives, the abundant hydroxyl groups on cellulose structures are substituted, so the inter-molecular hydrogen bonding is largely eliminated and the interaction with organic solvents is greatly enhanced.[183] To give an example, thermo-regulating ultrafine fibers based on the PEG/cellulose acetate (CA) composite were prepared by Chen *et al.*[182] Firstly, CA was dissolved in the mixture of *N*,*N*-dimethylacetamide and acetone, followed by the addition and mixing of PEG; secondly, electrospinning of the obtained solutions was performed and the wet fibers were vacuum dried. The prepared PCM composite fibers had a cylindrical shape and smooth surfaces, and PEG was distributed not only on the surfaces but also in the core of the composite fibers. The composite fibers showed high phase change enthalpies, and their thermal properties and morphologies remained almost unchanged after 100 heating/cooling cycles, indicating their reliability as thermo-regulating materials. Inspired by this, it is possible to use nanocellulose derivatives to fabricate composite phase change fibers. To this end, nanocellulose should be chemically converted to its ester counterpart by esterification reaction,[184] then the obtained nanocellulose derivatives can be incorporated into PCM solution for subsequential electrospinning. Nevertheless, this proposed method has remained unexplored so far.

A form-stable fiber-like composite PCM with cellulose fiber as the skeleton was obtained by Qu *et al.*[185] A eutectic mixture of PCMs myristic acid (MA) and tetradecanol (TD) was prepared by melt blending and ultrasonic dispersion, then the composite PCM was obtained by vacuum impregnation, in which the eutectic PCM entered the pores of cellulose fibers (Fig. 10(a)). As schematically shown, leakage prevention of the prepared composite PCM fiber was realized by physical interactions, including capillary force, surface tension and hydrogen bonding, that exist between PCM and cellulose. Through BET analysis, it was revealed that the pore structure is open-ended tubular capillary, which favors the capillary effect and makes absorption of PCM eutectics easier. The crystal structure of the TD-MA eutectic PCM was retained well after impregnation into fibers, and no chemical reactions occurred between PCM and cellulose. The presence of the PCM in the pores and on the surface of cellulose provided mechanical support to the eutectics, and porous cellulose fibers had a restriction function for the leakage of the liquid PCM during phase transitions. Thermal reliability analyses confirmed that the chemical structure and leakage prevention of this composite PCM were stable after 100 heating/cooling cycles. Alternatively, PCM molecules can be grafted onto the cellulose structure, resulting in composite PCM fibers. For example, a solid–solid composite PCM was developed by grafting PEG onto the cellulose backbone through urethane linkage by toluene 2,4-diisocyanate (TDI) for cooling application.[186] The PEG polymer was first dissolved in *N*,*N*-dimethylformamide (DMF), cellulose microcrystals were then added and mixed, followed by dropping TDI/DMF solution in the medium. The chemical reaction, induced by TDI, occurs among the hydroxyl groups of both PEG and cellulose. The results suggest that PEG grafting onto cellulose did not change the crystal form but limited the degree of crystallization; consequently a remarkable difference exists between the crystal structures of pristine PEG and PEG grafted cellulose composite PCM, evidenced by the polarized optical microscopy observations. The FTIR analysis confirms the formation of urethane and thus the success of the chemical reaction between PEG and cellulose. Importantly, the prepared composite PCM is stable after several thermal cycles, implying its potential use in LHS.

Nanocellulose and its functional hybrids have been utilized in the preparation of novel composite PCM nanofibers for advanced applications. For example, thermo/light-responsive CNC/zinc oxide (ZnO) nanohybrid phase change nanofibers (PCFs) for energy storage and regulated drug release were prepared by Abdalkarim *et al.*[187] In their previous studies, CNC/ZnO nanohybrids were utilized as nanofillers in poly(3-hydroxybutyrate-*co*-3-hydroxy-valerate) (PHBV) to enhance the mechanical, thermal, antimicrobial and UV shielding performances for wound dressing.[189,190] Herein, CNC/ZnO nanohybrids were used as versatile reinforcing agents to provide good shape and thermal stability/conductivity to PCFs, while the PCM realized the ''on–off'' temperature regulation of drug release. CNCs were prepared by the acid hydrolysis of microcrystalline cellulose, then CNC/ZnO nanohybrids were obtained *via* a one-step hydrothermal process with CNC as a carrier.[190] The electrospinning solutions were prepared by mixing PEG in a dichloromethane/DMF eutectic solvent, and PHBV was added as the supporting material. Meanwhile, PEG acted as the compatibilizer between CNC/ZnO nanohybrids and PHBV through hydrogen bonding with the two, ensuring the dispersibility and compatibility of the CNC/ZnO nanohybrid within the PHBV matrix. The composition of the electrospinning solution and the electrospinning process are schematically shown in Fig. 10(b). The prepared hybrid PCM fiber could release the drug above the melting temperature of PEG, while the drug release was suppressed below the melting temperature

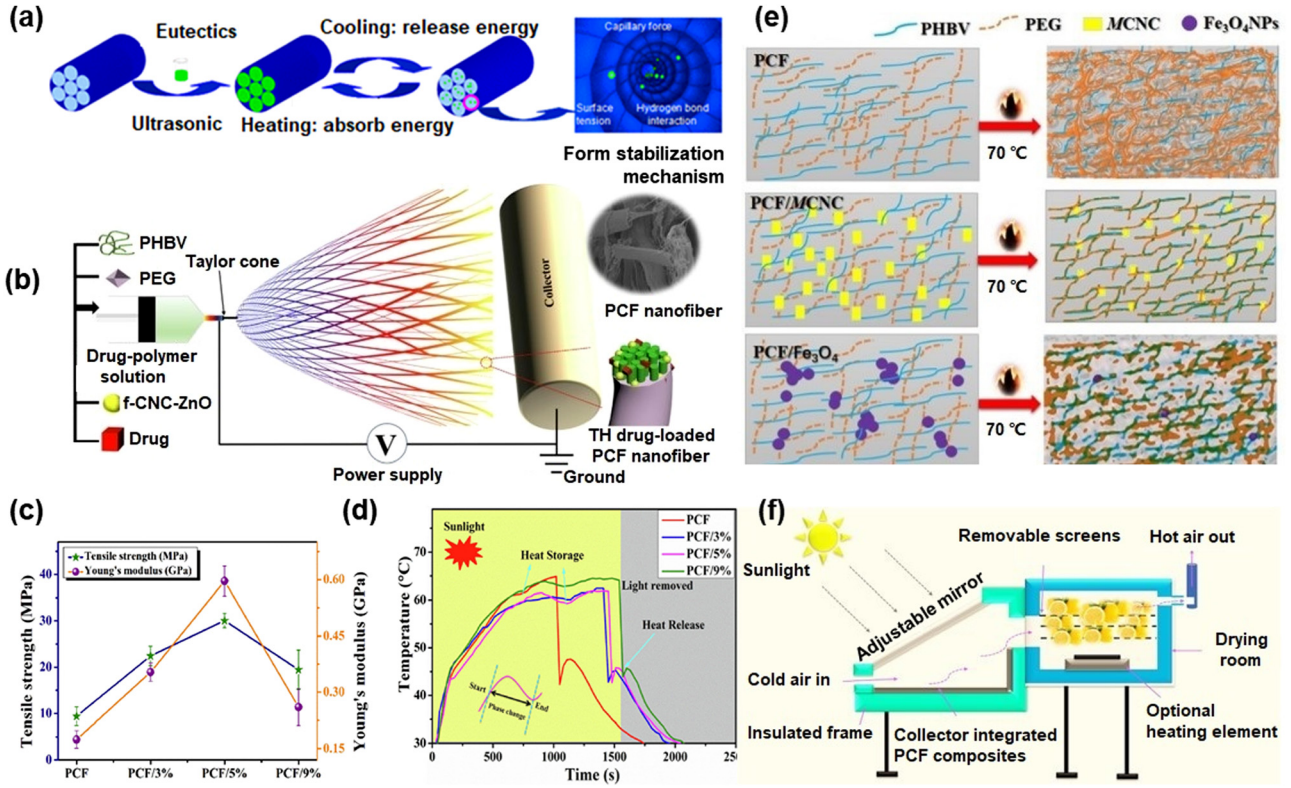

Fig. 10 (a) Schematic illustration of the preparation process of the myristic acid/cellulose composite PCM and the form stabilization mechanism therein, adapted with permission from ref. 185, Copyright 2017, Akadémiai Kiadó, Budapest, Hungary; (b) diagram of electrospinning solution composition and the possible electrospinning process for preparing the composite PCF encapsulated with CNC–ZnO, (c) tensile strength and Young's modulus of the composite PCF with various contents of CNC–ZnO, (d) temperature variations of the composite PCF with various contents of CNC–ZnO under solar irradiation at 100 mW cm^{-2} intensity, the inset shows the tangential method for determining the starting and ending points of the phase change period, reproduced with permission from ref. 187, Copyright 2019, Elsevier B.V.; (e) proposed mechanism for form stability of the magnetic/solar light-driven composite PCF under thermal treatment at 70 °C, and (f) schematic showing the solar dryer device based on the composite PCF for indoor and outdoor applications for fruit preservation and drying, reproduced with permission from ref. 188, Copyright 2020, Elsevier Ltd.

of PEG due to the barrier performance of a solid matrix. As shown in Fig. 10(c), the obtained PCF containing 5% of hybrid nanofillers exhibited considerably enhanced Young's modulus (241.7% increment) and tensile strength (219.5% increment) over the neat PCF. The mechanical enhancement can be attributed to the strong interactions between CNC–ZnO fillers and PCF, the formation of more uniform and finer fibers by introduction of CNC-based fillers, and the efficient stress transfer from the PCF to CNC–ZnO fillers. However, when the dosage of this nanofiller is more than 9%, the maximum values of mechanical strength start to decrease due to the possible agglomeration of nanofillers. PCFs with nanofillers also displayed enhanced thermal stability, thermal reliability and reusability, which are favorable for thermal energy storage. In the photothermal heat conversion testing of the PCF composites (Fig. 10(d)), temperature inflection points close to the phase transition temperature of the PCF composites indicate that the composite PCM absorbed the irradiated light and converted it into thermal energy, which was then stored in the PCM. Moreover, the increased amounts of CNC–ZnO fillers led to higher composite temperature and extended the energy storage period. When the light source was removed, the temperature of composite PCMs dropped rapidly and the stored energy was released during the phase change process.

Recently, CNC–Fe_3O_4 hybrids (MCNC) were used to prepare PCFs for dipole stimuli-responsive magnetic/solar light-driven energy conversion and storage.[188] PCFs were facilely fabricated by electrospinning of the PEG/PHBV/MCNC mixture, among which MCNC was synthesized by the coprecipitation method. Interconnecting bonds exist between the randomly distributed PCFs, preventing the possible PEG leakage issue. In the shape stability testing, both neat PCF and composite PCF containing 5% of MCNC did not suffer from the leakage problem during heating. The proposed mechanism is schematically presented in Fig. 10(e), *i.e.* the porous structure of PHBV, strong hydrogen bonding interactions between PCF and MCNC fillers and PEG diffusion *via* the 3D-nonwoven structure with interconnecting bonds together contributed to the shape stability of composite PCFs with nanocellulose-based fillers. However, PEG leakage was visible in the composite PCF containing 5% of Fe_3O_4, which is ascribed to the lack of the supporting matrix and interactions between the components. Besides the improved shape stability, the as-prepared composite PCFs exhibited superior phase change performance (latent heat of

69.2 ± 3.5 J g^{-1}–83.1 ± 4.2 J g^{-1}), excellent thermal stability, thermal reliability and durability, indicating their promising use for TES applications. Moreover, MCNC hybrids can be significantly stimulated with an alternating magnetic field and sunlight irradiation, leading to highly efficient thermal energy conversion, storage and application. An example of applying the composite PCFs for magnetic (indoor) and solar (outdoor) dryers for agricultural products like fruits is graphically shown in Fig. 10(f), contributing to the totally green heating process for production.

4.4 Nanocellulose-based composite PCM films

The structural rigidity of conventional PCMs remains a major bottleneck that results in poor surface contact with integrated devices and ultimately limits real scale applications.[191] Several methods are available to prepare flexible composite PCMs, among which fabricating composite PCM films or membranes using a flexible supporting matrix is simple and effective.[192] During film preparation, multifunctional materials such as photothermal agents can be integrated to obtain versatile composite PCMs. For example, a form-stable and flexible PCM composite film composed of the polydopamine–polyurethane polymer matrix and PEG was reported by Tas *et al.*[193] Waterborne polyurethane (WPU) particles were coated with polydopamine (PDA) to obtain the polymer matrix, followed by adding PEG into the PDA-WPU dispersion to form the final composite for film casting. The thermal stability and thermal conductivity of the amorphous polymer matrix were improved by its semicrystalline character induced by PEG addition. Although the tensile strength and elongation at break of composite films decreased when increasing PEG contents, the films still remained flexible. The prepared form-stable, flexible, and durable composite films did not suffer from PCM leakage and their phase change enthalpies remained constant after 60 heating/cooling cycles, fulfilling their application in solar-to-thermal energy conversion and storage with a conversion efficiency of 72.9%.

Owing to its sustainability and multifunctionalities, nanocellulose can be used for the preparation of advanced composite PCM films. For example, with the use of carboxylated nanocellulose, Shi *et al.* prepared poly (ethylene oxide) (PEO)-based PCM composite films.[194] These films were prepared by simply mixing carboxylated CNF dispersion and PEO solution at different mass ratios, followed by casting and drying steps. TEMPO-modified CNFs were used since their higher aspect ratio over CNCs and their good dispersion in hydrophilic PEO solution contribute to excellent reinforcement of the composite films. When increasing the CNF loading content from 0% to 20%, the density, moisture content and light transmittance of the films increased. Interestingly, the pure PEO film is translucent while the composite containing 20% of CNF is transparent (Fig. 11(a)), making its possible applications in optics. As presented in Fig. 11(b), inside the pure PEO film, large PEO spherocrystals with high crystallinity formed plenty of heterogeneous crystal interfaces that favor diffuse light reflection. When raising CNF content in composite films, for example to 20%, the amount of PEO spherocrystals decreased, consequently increasing light transmittance through the film. Due to the uniform dispersion of CNFs and the formation of hydrogen bonds at the interfaces between CNFs and PEO, the composite PCM film exhibited remarkably improved Young's modulus (0.2 to 2.4 GPa, 11 fold) and tensile strength (6 to 86 MPa, 14 fold) over the neat PEO film. Furthermore, CNF addition restricted the thermal expansion of composite films at temperatures above the melting point of PEO, ensuring their shape-stability for practical uses. Fukuya *et al.* investigated the changes in the crystallite orientation of the PEO/CNF composite film depending on CNF addition,[195] and the proposed mechanism is schematically presented in Fig. 11(c). In particular, when CNF content is less than 10% (based on weight of film), the molecular chains in the PEO crystallite region are oriented in a direction perpendicular to the film surface; when CNF content is more than 50%, the PEO molecular chains were oriented parallel to the film surface. The CNFs become parallel to the composite film surface when CNF content is more than 25%. The authors suggested that the hydrogen bonds between PEO and CNFs may behave as crystallization nuclei for PEO, and the space for PEO crystallization would be suppressed when increasing the CNF content in the composite film and consequently change the orientation of PEO crystals. In short, the change in the PEO crystallite orientation is due to the space between individual CNFs and the hydrogen bonds between CNF and PEO, which can be facilely tuned by controlling the CNF content introduced to the composite film. Their findings shed light on the development of PCM films that are more impermeable to gases for certain special applications, *e.g.* smart and protective packing. Li *et al.* fabricated a PCM film with superior mechanical performance using CNF-capsulated paraffin that was prepared *via* the Pickering emulsion technique.[196] CNFs with high aspect ratios act as the high-strength matrix as well as the stabilizer for the emulsion, and their strong capability to form an entangled network inside the composite film could absorb some stress and enhance the mechanical strength of the composite film. During the heating/cooling cycles, the composite PCM film exhibited reasonable enthalpy and thermal regulation properties without PCM leakage. Owing to the abundant hydroxyl groups of CNFs, this PCM film has the advantage of higher water absorption/retention, which makes its outdoor applications (*e.g.* smart building) possible.

A bio-based flexible PCM composite film with superior thermal conductivity was reported lately.[197] The preparation of the PEG-based phase change film is schematically illustrated in Fig. 11(d). First, the PCM component was held in the porous expanded graphite (EG) *via* vacuum absorption, then the obtained PEG/EG hybrid was mixed with CNFs that act as the film-forming substance and supporting matrix, followed by the incorporation of thermal conductivity enhancer boron nitride (BN). The combined use of EG and nanocellulose provided shape-stability to the composite film, and the as-prepared film can be easily rolled, showing excellent flexibility. The PEG/EG/CNF composite film also displayed improved

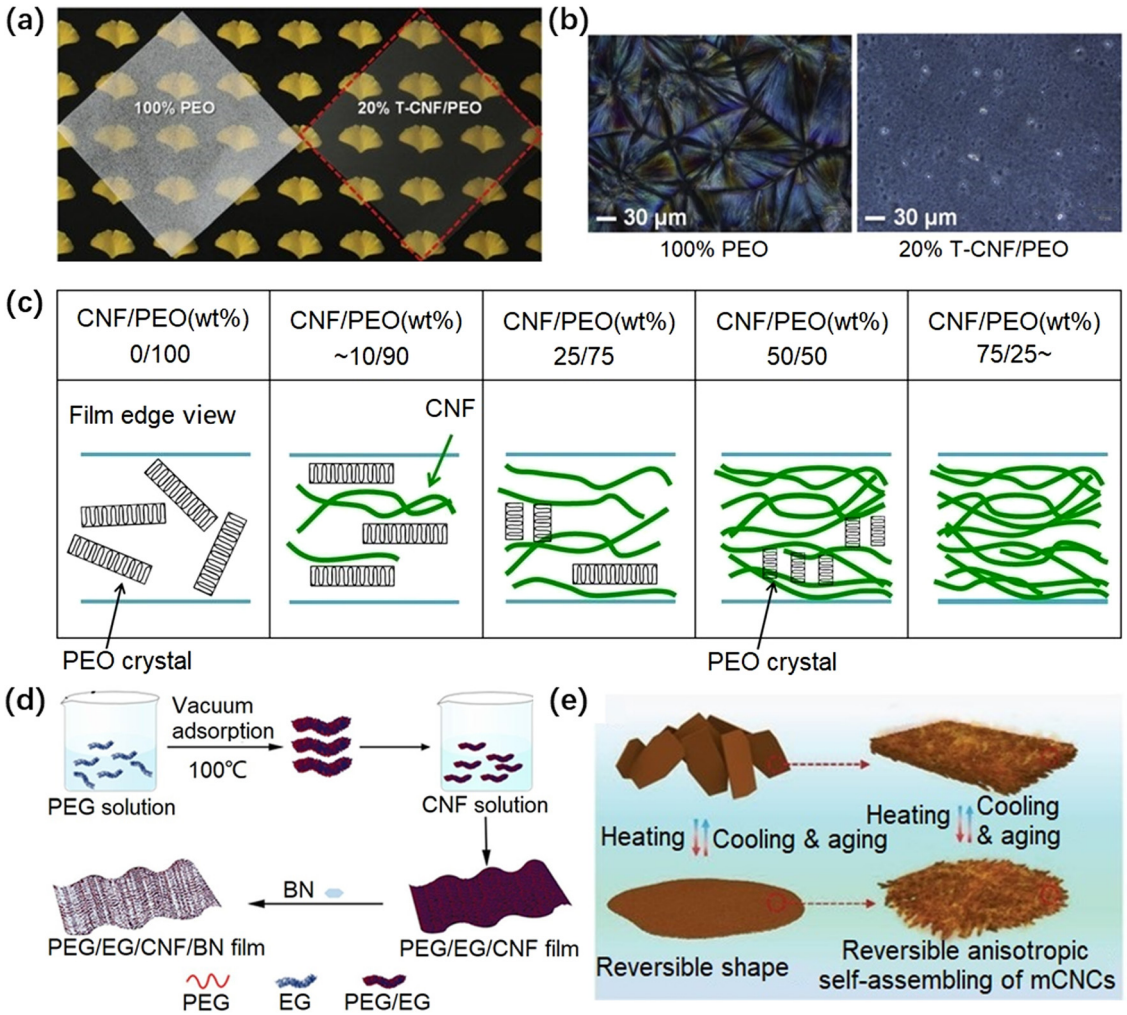

Fig. 11 (a) Photographs of the pure PEO film and the PEO composite PCM film containing 20% of CNF, (b) polarized optical microphotographs of the pure PEO film and the PEO composite PCM film containing 20% of CNF, adapted with permission from ref. 194, Copyright 2019, Elsevier Ltd.; (c) preferred PEO crystalline structures from the edge-view of PEO/CNF composite films, reproduced with permission from ref. 195, Copyright 2017, American Chemical Society; (d) flow chart of the preparation of the PEG/EG/CNF/BN composite PCM film, adapted with permission from ref. 197, Copyright 2021, Elsevier Ltd.; (e) schematic showing the formation of a thermo reversible flaky structure based on PCMs and CNCs, adapted from open source under the CC BY-NC license.[198]

thermal conductivity as graphite itself has excellent thermal conduction performance. Interestingly, this film showed anisotropic thermal conduction performance due to the highly aligned lamellar structure. Specifically, the radial thermal conductivity continuously increases with increasing EG content while the axial thermal conductivity remains unchanged. When BN was added at a certain EG level, the PEG/EG/CNF/BN composite film also exhibited anisotropic thermal conduction performance as the aligned BN fillers enter the lamellar structure of the composite film. When 7% EG and 15% BN were incorporated, the thermal conductivity of the composite film was improved by 3384% (radical) and 500% (axial) compared to that of the pure PEG film, respectively. The obtained PCM film also displayed satisfactory phase change performance and thermal stability, suggesting its promising use in thermal management of electronic devices.

New approaches for preparing composite PCM films or sheets are emerging. To give an example, a series of PCM composite nanofibrous mats consisting of PEO and CNCs were fabricated by an electrospinning method.[199] The microstructures of the composite films can be altered from the homogeneous state to heterogeneous state by changing the concentration of the electrospinning solution. When increasing the addition level of CNCs, the electrospun nanofibers became finer and more uniform, which can be attributed to the improved electric conductivity of the electrospinning solution. The size uniformity of the obtained PCM fibers was enhanced by the reducing needle diameter. The high alignment, uniform dispersion of CNCs and their strong interactions with PEO molecules *via* hydrogen bonding enabled the effective stress transfer from PEO to CNCs, leading to enhanced mechanical performance of the obtained PCM mats. Moreover, the

heterogeneous PCM mats containing rigid–flexible bimodal nanofibers provided better mechanical properties over the homogeneous counterparts at all CNC addition levels (0–20 wt%). The proposed mechanism is that the secondary ultrafine nanofibers in the heterogeneous structure associated strongly with primary nanofibers through their bonding points and inter-entanglement between them. However, homogeneous mats lack entangling secondary ultrafine fibers, leading to less inter-fiber interaction and thus inferior mechanical performance. Liu *et al.* investigated the thermal stability enhancement of polyurethane films by adding CNCs.[200] In their work, composite films with 1–5% of CNCs were prepared by a solvent casting method. It was found that the stiffness, strength and elongation of the film remained unaffected while the thermal degradation temperature increased, which indicates the enhanced thermal stability of the composite film. The higher onset decomposition temperature by 1% CNC addition was believed to be related to the hydrogen bonds between the hydroxyl groups of CNCs and urethane groups. When increasing the CNC content to 5%, the elastic modulus of the composite film was increased by about 70% without compromise of film elongation at break, revealing that CNCs did not prevent the flow or sliding of the hard blocks of polyurethane while they restricted the mobility of the soft segment, and CNCs themselves can move freely in tensile operation. Regardless of the addition levels of CNCs, all composite films had similar enthalpy values in the heating and cooling process; however, the crystallization temperature of the films shifted to higher temperatures when increasing the CNC content. The authors suggested that dispersed CNCs in the system behaved as the nucleating sites that favored the crystallization process and led to the elevated crystallization temperature. Their research confirmed the capability of CNCs in enhancing the thermal stability and crystallization efficiency of composite PCM films, although their mechanical reinforcing effect was inferior to that of CNFs. Malmir *et al.* studied the effect of CNC addition on the morphological, thermal, crystallization and barrier properties of the solution casting prepared PHBV/CNC composite film.[201] It was verified that CNCs acted not only as the bridges for connecting PHBV chains and cover the pores but also as the nucleating agent for PHBV crystallization. Compared to the neat PHBV film, the freezing of the composite PCM film started earlier and continued with a higher rate without changes in the crystalline structure of PHBV. Nevertheless, excessive addition of CNCs may restrict the free mobility of PHBV chains and result in slower growth of spherulites, and lead to the formation of porous film morphology. Notable improvement in the barrier performance against water vapor and oxygen was discovered and this can be attributed to the modified crystallinity of the composite film and the tortuosity effect by CNC fillers.

Nowadays, stimuli-responsive materials with highly ordered and reversible structures have gathered tremendous interest for their novel applications. As a proof of concept, Yang *et al.* engineered multifunctional reversible self-assembled structures of the CNC-derived phase change film.[198] In their design, PCMs act as temperature-responsive materials, and by adjusting their interactions with nanoparticles (*e.g.* van der Waals forces, dipole–dipole interactions and hydrogen bonding) during phase transitions, both energy storage and self-assembled structures can be achieved. For this purpose, phase change nanocrystals (PCNs) were prepared by anchoring 1-octadecanethiol PCM onto esterification modified CNCs through thiol-ene reaction, and the PCNs had a hard CNC core that retained the basic structure and a soft shell of phase change octadecyl chains. Their unique structure and the phase change behavior of the shell allowed the self-assembly of the PCNs into well-ordered reversible hierarchical structures. As shown in Fig. 11(e), the self-assembled nano/micro structure forms a flaky or film like morphology when being heated, and the original structure can be recovered by a cooling and aging process. During the reversible structure and morphology switch, the formation of the flaky structures is ascribed to the ordered organization of modified CNCs by molecular interactions between octadecyl chains that results in the crystalline structure within the film. Specifically, after heating at 80 °C the modified CNCs become isotropic because of the dissociation of the crystalline domains of the packed octadecyl chains. Nanoflakes with crystalline texture were generated by modified CNCs when decreasing the temperature to 25 °C and aging for further 24 h. Moreover, this phase change film exhibits self-healing and thermally reversible properties like birefringence, hydrophobicity and transparency. These amazing properties impart possible application in smart surfaces, thermal sensitive imaging and temperature-preserving coatings.

4.5 Nanocellulose-based composite PCM blocks

As introduced earlier, nanocellulose foams and aerogels can be facilely prepared by freeze drying and supercritical drying, and these porous materials usually have low density, high prosody, large specific area, and favorable mechanical performance. Manipulating the chemistry of nanocellulose gives a chance for fabricating compatible scaffolds for different types of PCMs. Undoubtedly, porous nanocellulose-based scaffolds have found their application in preparing form-stabilized and leakage free composite PCMs, and multifunctional composites can be achieved when the corresponding fillers are incorporated in the preparation of nanocellulose-based supporting materials.

A form-stable PCM composite with improved thermal conductivity by using alkylated CNF/carbon nanotubes (CNTs) aerogels as the scaffold was reported by Du *et al.*[202] In their work, alkylated composite aerogels were prepared by cation induced gelation of the CNF/CNT suspension, followed by the freeze-drying and surface modification steps. In particular, the alkylation modification was performed for improving the compatibility between the prepared composite aerogels and *n*-octacosane PCM. The PCM composites were obtained by impregnating the aerogels with molten PCM in vacuum. Morphology observations proved that all the aerogels have well oriented and interconnected multiporous structures, which favor the absorption of PCM liquid. Due to the enhanced compatibility between the supporting aerogel and PCM,

composite PCMs have high loadings of *n*-octacosane and compact internal structures without clear interfaces between the components. The leakage issue was completely resolved due to considerable capillary force and surface tension, and composite PCMs exhibited form stability even when being heated at 80 °C for 60 min. The thermal conductivity of composite PCMs was effectively increased from 0.247 to 0.583 W (m^{-1} K^{-1}) by CNT introduction. The high phase change enthalpy (maximum 252.9 Jg $^{-1}$), favorable form stability and excellent thermal stability and reliability favor their applications for energy storage. Due to the superior photo-thermal conversion ability of CNTs, the as-prepared composite PCMs exhibited promising potential in solar-thermal conversion and storage application, with the photo-thermal conversion and storage efficiency improved from 46.9 to 83.4%. Similarly, Shen *et al.* used CNF/CNT composite foam to fabricate form-stabilized composite PCMs for solar-thermal-electrical storage and conversion.[203] To improve the compatibility between the foam scaffold and paraffin PCM, CNF-based foams were hydrophobically silylated with methyltrimethoxysilane. The authors studied the relations between foam density and porosity, and their effects on the paraffin absorption capacity of foams and leakage ratio of composite PCMs. Conclusions are drawn that higher concentration of the CNF-based suspension for foam preparation leads to denser and less porous foams with smaller pores, and this results in slightly decreased paraffin loading ability but enhanced leakage prevention. The good compatibility of silylated CNF/CNT foams with paraffin was verified by the absence of clear interfaces inside the composite PCMs, and no chemical reaction was detected between the foams and paraffin. The good form-stability, negligible leakage during phase transitions, and thermal stability and reliability favor the application of composite PCMs for realistic applications. Moreover, the use of CNTs obviously enhanced the heat transfer properties of PCMs and their solar harvesting and energy conversion efficiency.

To improve the energy storage density and thermal stability of the octadecanol (OCO)/octodecane (OCC) PCM, CNF/silver nanowire (AgNW) hybrid porous foam with a highly ordered structure was utilized as the supporting material.[204] CNFs were prepared by TEMPO-oxidation of the decolorant wood powder to avoid aggregation of nanofibers, and long and thin AgNWs were obtained by simple hydrothermal synthesis,[205] followed by the mixing of two solutions to form CNF/AgNWs hybrids. Anisotropic composite foams were fabricated by directional freezing, and were then impregnated with the molten PCMs to obtain the composite foam-supported PCMs (Fig. 12(a)). Interconnected cellulose-based foams with uniform porous morphologies in the perpendicular cross-section and pyknotic hexagonal honeycomb porous structure in the horizontal cross-section were observed, and their color was dependent on the AgNW content, which can be attributed to improved light absorption by the synergy effects of light absorption performance of AgNWs and the 3D foam scaffolds. Composite foams were also prepared by a non-directional freezing method, and their porous structure was uniform in both horizontal and perpendicular cross-sections; however, the AgNW content decreased in these foams, indicating the advantage of directional freezing in preparing anisotropic cellulose-based structures with uniform filler dispersion. Owing to the numerous hydroxyl groups of the supporting foam, an ultrahigh loading level of the OCO PCM was enabled by intensive hydrogen bonding and higher enthalpy was imparted to this composite PCM compared to the OCC composite PCM, which is ascribed to the interfacial hydrogen bonds of the former. The prepared OCO-based composite PCM exhibited distinguished shape, chemical and thermal stability. Thermal conductivity measurements and infrared images verified the improved heat transfer capacity over the pure OCO, and the proposed mechanism is presented in Fig. 12(b). Specifically, the synergistic effects of the AgNW presence and strong interfacial interactions facilitated the phonon propagation for heat transfer. Due to the addition of AgNWs and the advantage of the directional freeze-drying induced highly ordered structure, the prepared composite PCMs showed greatly improved heat transmission in the longitudinal direction than in the transverse direction. These good merits suggest their promising applications in high-efficiency solar-thermal energy conversion and storage and anisotropic thermal transmission. In the research by Xue *et al.*,[206] the CNF/GNP solution was used to impregnate melamine foam (MF), followed by the oriented freezing of the MF/CNF/GNP composite, freeze drying and carbonization processes. Owing to the strong hydrophobic–hydrophobic interactions between CNFs and GNPs and the intensive hydrogen bonding between CNFs and MF, CNFs function as a bridge between MF and GNPs. Compared to the conventionally anisotropic GNP aerogel-stabilized PCM, the MF/CNF/GNP hybrid foam-stabilized paraffin PCM is oriented in both horizontal and perpendicular directions. The prepared composite PCMs displayed improved form-stability, thermal conductivity, thermal stability and cycling reliability. Different from the conventional applications like photo-thermal conversion and storage, the prepared composite PCMs were used for electric-to-thermal transition application. The experimental design of a delay switch to control the illumination of a bulb is presented in Fig. 12(c). The measured current through the sample (Fig. 12(d)) obviously increased when the voltage is applied and this is related to the rearrangement of GNPs during the melting process of paraffin induced by Joule heating. The results also verify the fast response of composite PCMs to the electrification process and their excellent cycling stability. Digital images of the real application are presented in Fig. 12(e). Image I shows the bulb that is not lighted in 50 s, and image II shows the bulb which illuminates brightly in 420 s when voltage is applied. Their research opens up the novel applications of PCMs, such as electric-to-thermal conversions and microelectronic devices related to a delay switch.

CNF/polypyrrole (PPy) hybrid aerogel supported octacosane composite PCMs with form-stability and excellent energy storage performance were fabricated by Xu *et al.*[207] To improve the photo-thermal conversion capability of the PCMs, PPy was introduced onto the surface of the nanocellulose aerogel

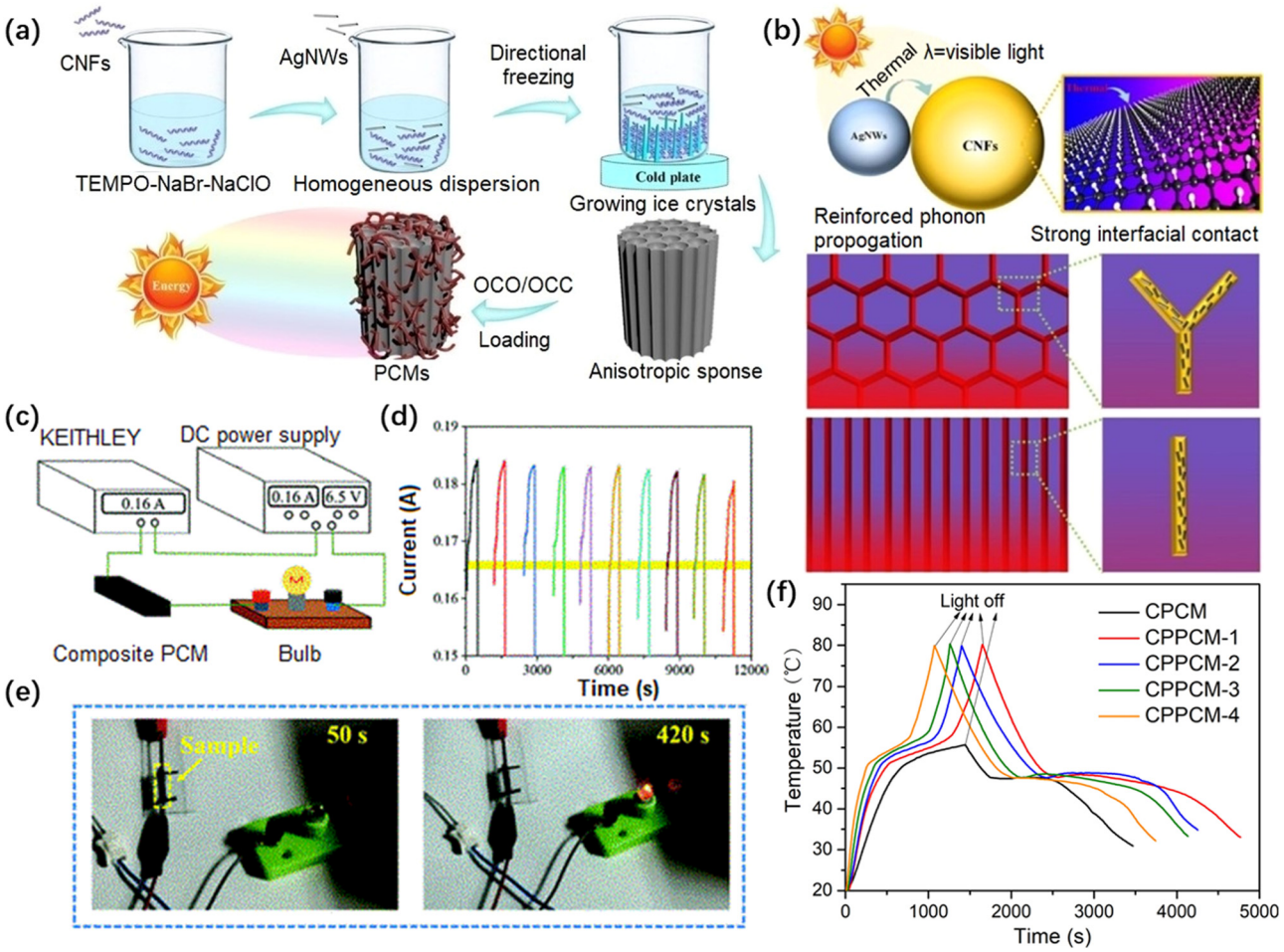

Fig. 12 (a) Schematic illustration of the preparation of anisotropic composite PCMs, (b) schematic diagram of the thermal transfer mechanism of the prepared composite sponges (upper), and the characteristic thermal conduction mechanism of the composite sponges along horizontal cross-section (middle) and perpendicular cross-section (lower), reproduced with permission from ref. 204, Copyright 2021, Elsevier B.V.; (c) schematic diagram of the delay switch experiment, (d) current change of the composite PCM depending on time, (e) photos of the state of the small bulb at different times when voltage was applied, reproduced with permission from ref. 206, Copyright 2020, Royal Society of Chemistry; (f) temperature of composite PCMs with time under sunlight irradiation of 300 mW cm^{-2}, adapted with permission from ref. 207, Copyright 2020, Springer Nature B.V.

support *via in situ* polymerization. The preparation of CNF/PPy aerogels consists of two steps: first, mixing of CNF aerogels with PPy and TsOH; second, *in situ* polymerization of PPy, followed by the freeze-drying process. The composite PCMs were fabricated by vacuum-aided impregnation of aerogels in melted PCMs. The typical porous microstructure of the composite aerogel and uniform distribution of PPy were discovered, and the porous structure with the capillary effect and the compatibility between aerogel support and PCM contributed to a high loading fraction of *n*-alkane. Due to the substitution of the PCM with other components (*i.e.* CNF and PPy), a reasonable reduction (5%) in phase change enthalpy was found, as reported elsewhere.[203] Form-stability, thermal stability and reliability were confirmed during repeated heating/cooling cycles. When applied for solar-thermal conversion and storage, these composite PCMs showed improved photo-thermal conversion and storage efficiency (up to 86%), and the improvement is positively associated with the addition level of solar-thermal conversion material PPy (Fig. 12(f)). Moreover, increased PPy content accelerated the charging and discharging of composite PCMs, as evidenced by the narrower phase transition platform during heating and cooling. Similarly, a CNF/melanin hybrid aerogel was prepared and used to stabilize PEG and improve the photothermal conversion efficiency and energy storage density.[208] The same preparation strategies, *i.e.* freeze drying of the CNF-based mixture suspension and follow-up impregnation of aerogels with the molten PCM, were used to obtain the form-stabilized composite PCMs. The incorporated melanin imparted irregular protrusions on the pore wall structure, but the main porous scaffold structure remained unchanged, which prohibited the leakage issue during phase transitions. Meanwhile, the introduction of melanin remarkably improved the photo-thermal conversion efficiency from 47.2 to 85.9%, with the energy storage density of composite PCMs unaffected. The prepared composite PCMs also displayed satisfactory phase change and thermal properties,

favoring promising solar-thermal conversion and storage applications.

Novel composite PCMs based on a CNF/graphene hybrid aerogel and PEG were fabricated by Du *et al.*[209] To improve the affinity of the CNF-based aerogel with the PEG PCM, grafting of PEG molecules onto CNFs was performed *via* carboxylation–amidation reaction. The chemically modified CNFs were then mixed with graphene oxide (GO), followed by the chemical reduction of GO to graphene and aerogel preparation by freeze-drying. The as-prepared hybrid aerogels had 3D interconnected porous structures that well encapsulated the PCM and prevented its leakage. Due to the enhanced affinity between the aerogel support and PCM, the resulting composite PCM exhibited greatly improved loading levels of PEG and satisfactory shape stability. Graphene as a thermal conduction filler greatly enhanced the thermal conductivity of the PCM and imparted promising photo-thermal conversion and storage performance to the composite PCM. Their study gives some inspiration for using PCM molecules to modify the supporting materials for improved affinity between the two. In recent work, CNC/GNP/PEG composite PCMs were prepared through a simple physical compounding method.[210] Specifically, CNCs and GNPs were dispersed and sonicated in deionized water and ethanol, respectively, followed by mixing of the two dispersion and the addition of PEG. The obtained mixture was then cast and vacuum dried to prepare the composite PCMs. CNCs not only enabled good dispersion of GNPs *via* their amphiphilic nature but also provided strong encapsulation of the PCM *via* their hydrogen bonding with PEG. These prepared composite PCMs showed a stable form, greatly improved thermal conductivity, high latent heat and favorable thermal energy conversion capability, showing great potential for ensuring the normal operation of electronic devices when combined with a thermally sensitive switch. Therefore, it is safe to conclude that nanocellulose-based hybrid supporting materials can provide shape-stability and versatile functions to PCMs, especially when combined with multifunctional materials like thermal conductivity fillers and photosensitive and thermal sensitive additives. The resulting composite PCMs are expanding their applications from conventional thermal energy storage to intelligent thermal management systems.

5. Summary and outlook

Thermal energy storage as one of the most effective techniques to expand the use of sustainable energy has been considered as a possible solution to energy issues and environmental pollution. By storing surplus heat and using it at a later time, thermal energy storage provides several advantages, such as economic benefits, peak load shifting, high energy utilization efficiency and energy reliability. Compared to sensible heat storage and thermochemical heat storage, latent heat storage shows merits like higher energy storage density, small temperature swings in heat storage and release, simple operation and low investment and thus is preferred for TES system fabrication. PCMs are the core component of TES systems and store and release heat at a fixed temperature during their phase transitions, but are subject to the drawbacks of liquid leakage, low thermal conductivity, phase separation, supercooling and insufficient thermal and cycling stability for scalable applications. Fabricating sustainable high-performance composite PCMs meets the growing demand for renewable energy storage and help address environment concerns, which has been one of the hottest topics in latent heat storage and utilization.

Nanocellulose as a fascinating and versatile material derived from the most abundant natural polymer on earth has provoked intense attention from both academia and industry, and exhibits the merits of renewability, biodegradability, recyclability and ease of functionalization. With optimization, nanocellulose can be integrated into PCMs to prepare composite slurries, capsules, fibers, films and blocks to tackle the existing drawbacks of PCMs. Firstly, by incorporating nanocellulose and nanocellulose-based hybrids, salt hydrate PCM slurries with a stable phase, less supercooling and higher thermal conductivity can be obtained. In this scenario, nanocellulose behaves as the thickening agent *via* its excellent networking capability, and as a stabilizer/support for nucleating nanoparticles and carbon nanomaterials. Nanocellulose with a high aspect ratio and suitable surface environment, *e.g.* pristine CNFs, benefits its application for preparing composite PCM slurries. Secondly, when used for the preparation of composite PCM capsules, CNFs and CNCs are typically used as the stabilizers of the emulsion, shell forming materials or reinforcing agents of the shell structure. Chemical modification of nanocellulose can be performed to optimize its compatibility during polymerization and improve the performance of composite PCMs. Thirdly, composite phase change fibers can be fabricated by directly immobilizing PCM molecules onto the fiber surface and backbone or by electrospinning of nanocellulose/PCM mixtures. In this case, nanocellulose may act as the backbone of the composite, the strengthening agent for composite PCM fibers, and the carrier of functional nanoparticles. Fourthly, nanocellulose-based composite PCM films can be fabricated by various techniques, such as simple solution casting, coating or impregnation of the nanocellulose film with molten PCMs. The use of nanocellulose provides a way to prepare flexible and strong composite PCM films with tunable optical and thermal properties. Fifthly, to prepare form-stable composite PCM matrices, nanocellulose-based foams and aerogels can be used as the porous supporting materials, in which modified nanocellulose or functional materials can be incorporated for compatible, durable and multifunctional cellulosic scaffolds. These composite PCM blocks are usually fabricated by impregnation of porous nanocellulose-based porous scaffolds with liquid PCMs with the aid of vacuum. Due to the high liquid absorption capacity of nanocellulose-based scaffolds and their favorable interactions with the PCM, the prepared PCM composites usually have compact structures and a stable phase during phase transitions.

Based on the intrinsic structural and surface properties of nanocellulose, its thickening effect for salt hydrate inorganic

PCMs stemmed from the physical entanglements of cellulose nanofibers that prevents salt precipitation, and nanocellulose-supported nanoparticles can facilitate the salt crystal growth on their surfaces and decrease the supercooling degree of salt hydrates. Importantly, the abundant hydroxyl groups of nanocellulose contribute to its compatibility with salt hydrate PCMs, and these functional groups of nanocellulose also benefit its chemistry manipulation *via* various strategies, *e.g.* grafting onto and grafting from. The amphiphilicity feature of nanocellulose benefits the exfoliation and dispersion of carbon nanomaterials like graphene. As a result, the nanocellulose/nanocarbon hybrid with favored dispersion can be used to prepare thermally stable composite PCMs with enhanced thermal conductivity. Due to the stress transfer and distribution effect, the use of nanocellulose could enhance the mechanical performance of the prepared composite PCM capsules, fibers, and films. Besides being used as additives, nanocellulose can also behave as the skeleton of composite PCMs due to the strong interactions between the cellulose nanoparticles or nanofibers. These interactions include self-entanglement (for CNFs) and hydrogen bonding. When porous nanocellulose scaffolds are used for encapsulation of PCMs, again, the compatibility, structures and properties of nanocellulose scaffolds could be facilely tuned by chemical modification or introducing nanocellulose-based hybrids. All in all, nanocellulose with fascinating chemistry and structural properties can serve as either a supporting skeleton or a functional additive for composite PCMs, suggesting its promising applications in fabricating sustainable and advanced composite PCMs for thermal energy storage and management.

Challenges, however, exist when applying nanocellulose for PCM-based TES applications. First, the efficiency, energy consumption and environmental impacts of nanocellulose preparation must be optimized, which can be done through effective pretreatment of starting materials by green chemistry or enzymes. With high efficiency production that is easily scaled up in industry, the commercialization and marketability of nanocellulose are expected to be boosted, which will enhance the cost-effectiveness of using this material. Second, some intrinsic characteristics of cellulose materials such as their hydroscopic nature, thermal instability and incompatibility with hydrophobic polymers should be overcome in their use, and this can be fulfilled by surface chemistry or introducing other functional substances. With delicate modifications, thermally stable cellulose materials that are capable of compositing with more types of PCMs can be prepared. Third, the performance of nanocellulose-based matrices should be improved for better structural and physicochemical properties of the prepared nanocellulose-based composite PCMs. For example, the strength, compression resistance and multifunction of nanocellulose-based porous scaffolds can be further enhanced to increase the uptake capacity of PCMs and meet the application requirement in designated environments. These improvements will prompt the performance and applicability of nanocellulose-based composite PCMs for different scenarios. Fourth, the reported nanocellulose-based composite PCMs are mostly prepared on a laboratory scale, and industrial level production is important for certain applications, such as smart building materials, thermal regulating textiles, and solar energy harvesting and conversion. Additionally, the application of certain nanocellulose structures like nanocellulose films and hydrogels has rarely been reported for TES applications and more research endeavor is needed. Last but not the least, more advanced composite PCMs (*e.g.* stimuli-responsive ones) for novel applications (*e.g.* biomedical uses) are desired. By means of this, both value-added applications of nanocellulose and utilizations of advanced PCM-based TES systems are to be expanded. Considering the ongoing research activities and rapid advances in science and technology, it would be safe to conclude that chances exist for the bright future of nanocellulose-based composite PCMs.

Conflicts of interest

There are no conflicts to declare.

Acknowledgements

This work was financially supported by the National Key Research and Development Program of China (2020YFA0210701) and the National Natural Science Foundation of China (51825201).

References

1 E. Borri, G. Zsembinszki and L. F. Cabeza, *Appl. Therm. Eng.*, 2021, **189**, 116666.
2 I. Dincer and M. Rosen, *Thermal Energy Storage: Systems and Applications*, John Wiley & Sons, Ltd, Chichester, UK, 2010.
3 P. Singh, R. K. Sharma, A. K. Ansu, R. Goyal, A. Sarı and V. V. Tyagi, *Sol. Energy Mater. Sol. Cells*, 2021, **223**, 110955.
4 B. Zalba, J. M. Marın, L. F. Cabeza and H. Mehling, *Appl. Therm. Eng.*, 2003, **23**, 251–283.
5 M. M. Umair, Y. Zhang, K. Iqbal, S. Zhang and B. Tang, *Appl. Energy*, 2019, **235**, 846–873.
6 S. Wu, T. Yan, Z. Kuai and W. Pan, *Energy Storage Mater.*, 2020, **25**, 251–295.
7 R. H. Pallinti Purushotham and J. Zimmer, *Science*, 2020, **369**, 1089–1094.
8 D. Klemm, B. Heublein, H. P. Fink and A. Bohn, *Angew. Chem., Int. Ed.*, 2005, **44**, 3358–3393.
9 J. S. M. Tavakolian Mandana and G. M. van de Ven Theo, *Nano-Micro Lett.*, 2020, **12**, 73.
10 D. Trache, A. F. Tarchoun, M. Derradji, T. S. Hamidon, N. Masruchin, N. Brosse and M. H. Hussin, *Front. Chem.*, 2020, **8**, 392.
11 Q.-F. Guan, Z.-M. Han, T.-T. Luo, H.-B. Yang, H.-W. Liang, S.-M. Chen, G.-S. Wang and S.-H. Yu, *Natl. Sci. Rev.*, 2019, **6**, 64–73.
12 Q.-F. Guan, H.-B. Yang, Z.-M. Han, L.-C. Zhou, Y.-B. Zhu, Z.-C. Ling, H.-B. Jiang, P.-F. Wang, T. Ma, H.-A. Wu and S.-H. Yu, *Sci. Adv.*, 2020, **6**, aaz1114.

13 H.-B. Yang, Z.-X. Liu, C.-H. Yin, Z.-M. Han, Q.-F. Guan, Y.-X. Zhao, Z.-C. Ling, H.-C. Liu, K.-P. Yang, W.-B. Sun and S.-H. Yu, *Adv. Funct. Mater.*, 2022, **32**, 2111713.
14 D.-H. Li, Z.-M. Han, Q. He, K.-P. Yang, W.-B. Sun, H.-C. Liu, Y.-X. Zhao, Z.-X. Liu, C.-N.-Y. Zong, H.-B. Yang, Q.-F. Guan and S.-H. Yu, *Adv. Mater.*, 2022, e2208098.
15 X. Du, Z. Zhang, W. Liu and Y. Deng, *Nano Energy*, 2017, **35**, 299–320.
16 F. Hoeng, A. Denneulin and J. Bras, *Nanoscale*, 2016, **8**, 13131–13154.
17 F. Li, E. Mascheroni and L. Piergiovanni, *Packag. Technol. Sci.*, 2015, **28**, 475–508.
18 A. Serpa, J. Velásquez-Cock, P. Gañán, C. Castro, L. Vélez and R. Zuluaga, *Food Hydrocolloids*, 2016, **57**, 178–186.
19 S. Salimi, R. Sotudeh-Gharebagh, R. Zarghami, S. Y. Chan and K. H. Yuen, *ACS Sustainable Chem. Eng.*, 2019, **7**, 15800–15827.
20 N. Mahfoudhi and S. Boufi, *Cellulose*, 2017, **24**, 1171–1197.
21 H. Luo, R. Cha, J. Li, W. Hao, Y. Zhang and F. Zhou, *Carbohydr. Polym.*, 2019, **224**, 115144.
22 J. H. Kim, D. Lee, Y. H. Lee, W. Chen and S. Y. Lee, *Adv. Mater.*, 2019, **31**, e1804826.
23 F. Jiang, T. Li, Y. Li, Y. Zhang, A. Gong, J. Dai, E. Hitz, W. Luo and L. Hu, *Adv. Mater.*, 2018, **30**, 1703453.
24 C. Liu, P. Luan, Q. Li, Z. Cheng, P. Xiang, D. Liu, Y. Hou, Y. Yang and H. Zhu, *Adv. Mater.*, 2020, **33**, 2001654.
25 J. Dai, M. Chae, D. Beyene, C. Danumah, F. Tosto and D. C. Bressler, *Materials*, 2018, **11**, 1645.
26 A. A. K. Das, J. Bovill, M. Ayesh, S. D. Stoyanov and V. N. Paunov, *J. Mater. Chem. B*, 2016, **4**, 3685–3694.
27 Y. Chu, Y. Sun, W. Wu and H. Xiao, *Carbohydr. Polym.*, 2020, **250**, 116892.
28 L. Urbina, M. Á. Corcuera, N. Gabilondo, A. Eceiza and A. Retegi, *Cellulose*, 2021, **28**, 8229–8253.
29 S. O. Dima, D. M. Panaitescu, C. Orban, M. Ghiurea, S. M. Doncea, R. C. Fierascu, C. L. Nistor, E. Alexandrescu, C. A. Nicolae, B. Trica, A. Moraru and F. Oancea, *Polymers*, 2017, **9**, 374.
30 C. Liu, B. Li, H. Du, D. Lv, Y. Zhang, G. Yu, X. Mu and H. Peng, *Carbohydr. Polym.*, 2016, **151**, 716–724.
31 H. Du, W. Liu, M. Zhang, C. Si, X. Zhang and B. Li, *Carbohydr. Polym.*, 2019, **209**, 130–144.
32 A. Blanco, M. C. Monte, C. Campano, A. Balea, N. Merayo and C. Negro, *Handbook of nanomaterials for industrial applications*, Elsevier, 2018, pp.74–126.
33 H. Xie, H. Du, X. Yang and C. Si, *Int. J. Polym. Sci.*, 2018, **2018**, 7923068.
34 O. Nechyporchuk, M. N. Belgacem and J. Bras, *Ind. Crops Prod.*, 2016, **93**, 2–25.
35 M. Ioelovich, in *Handbook of Nanocellulose and Cellulose Nanocomposites*, ed. H. Kargarzadeh, I. Ahmad, S. Thomas and A. Dufresne, John Wiley & Sons, Hoboken, New Jersey, U. S., 2017, vol. 1, pp. 51–100.
36 R. M. Domingues, M. E. Gomes and R. L. Reis, *Biomacromolecules*, 2014, **15**, 2327–2346.
37 A. Dufresne, *Mater. Today*, 2013, **16**, 220–227.
38 S. B. Robert Moon and A. Rudie, in *Production and Applications of Cellulose Nanomaterials*, ed. R. J. M. Michael, T. Postek, A. W. Rudie and M. A. Bilodeau, TAPPI Press, Peachtree Corners, GA, U. S. A., 2013, ch. 1, pp. 9–12.
39 R. J. M. Michael, T. Postek, A. W. Rudie and M. A. Bilodeau, *Production and Applications of Cellulose Nanomaterials*, TAPPI Press, Peachtree Corners, GA, U. S. A., 2013.
40 N. Lin, J. Huang and A. Dufresne, *Nanoscale*, 2012, **4**, 3274–3294.
41 S. M. S. R. A. Ilyas, R. Ibrahim, M. S. N. Atikah, A. Atiqah, M. N. M. Ansari and M. N. F. Norrrahim, in *Nanocrystalline Materials*, ed. B. Movahedi, IntechOpen, London, UK, 2020.
42 M. T. Islam, M. M. Alam and M. Zoccola, *Int. J. Innov. Res. Technol. Sci. Eng.*, 2013, **2**, 5444–5451.
43 S. Afrin and Z. Karim, *ChemBioEng Rev.*, 2017, **4**, 289–303.
44 H. Lee, J. Sundaram and S. Mani, in *Nanotechnology: Food and Environmental Paradigm*, ed. R. Prasad, V. Kumar and M. Kumar, Springer, Singapore, Singapore, 2017, pp. 1–33.
45 A. J. Benítez and A. Walther, *J. Mater. Chem. A*, 2017, **5**, 16003–16024.
46 Z. Fang, G. Hou, C. Chen and L. Hu, *Curr. Opin. Solid State Mater. Sci.*, 2019, **23**, 100764.
47 K. Zhang, P. Tao, Y. Zhang, X. Liao and S. Nie, *Carbohydr. Polym.*, 2019, **213**, 228–235.
48 G. H. Morales-Narváez Eden, N. Tina, Y. Hossein, K. Uliana, H. Daniel, P. Nahid and M. Arben, *ACS Nano*, 2015, **9**, 7296–7305.
49 A. Skogberg, S. Siljander, A.-J. Maki, M. Honkanen, A. Efimov, M. Hannula, P. Lahtinen, S. Tuukkanen, T. Bjorkqvist and P. Kallio, *Nanoscale*, 2022, **14**, 448–463.
50 W. Yang, Z. Zhao, K. Wu, R. Huang, T. Liu, H. Jiang, F. Chen and Q. Fu, *J. Mater. Chem. C*, 2017, **5**, 3748–3756.
51 C. N. Wu, Q. Yang, M. Takeuchi, T. Saito and A. Isogai, *Nanoscale*, 2014, **6**, 392–399.
52 Q.-F. Guan, Z.-C. Ling, Z.-M. Han, H.-B. Yang and S.-H. Yu, *Matter*, 2020, **3**, 1308–1317.
53 J. Yang, H. Xie, H. Chen, Z. Shi, T. Wu, Q. Yang and C. Xiong, *J. Mater. Chem. A*, 2018, **6**, 1403–1411.
54 Y. Li, H. Zhu, F. Shen, J. Wan, S. Lacey, Z. Fang, H. Dai and L. Hu, *Nano Energy*, 2015, **13**, 346–354.
55 K. Yao, Q. Meng, V. Bulone and Q. Zhou, *Adv. Mater.*, 2017, **29**, 1701323.
56 T. Bayer, B. V. Cunning, R. Selyanchyn, M. Nishihara, S. Fujikawa, K. Sasaki and S. M. Lyth, *Chem. Mater.*, 2016, **28**, 4805–4814.
57 D. Jiao, F. Lossada, J. Guo, O. Skarsetz, D. Hoenders, J. Liu and A. Walther, *Nat. Commun.*, 2021, **12**, 1–10.
58 Q.-F. Guan, K.-P. Yang, Z.-M. Han, H.-B. Yang, Z.-C. Ling, C.-H. Yin and S.-H. Yu, *ACS Mater. Lett.*, 2022, **4**, 87–92.
59 Q.-F. Guan, Z.-M. Han, H.-B. Yang, K.-P. Yang, Z.-C. Ling, C.-H. Yin, Y.-X. Zhao, J.-L. Wang, B.-B. Yan, T. Ma, B.-C. Hu, C. Li, X.-F. Pan, S.-M. Chen, S.-Y. Ma and S.-H. Yu, *Adv. Mater. Technol.*, 2021, **6**, 2100193.
60 M. Pääkkö, M. Ankerfors, H. Kosonen, A. Nykänen, S. Ahola, M. Österberg, J. Ruokolainen, J. Laine, P. T. Larsson and O. Ikkala, *Biomacromolecules*, 2007, **8**, 1934–1941.

61 E. E. Ureña-Benavides, G. Ao, V. A. Davis and C. L. Kitchens, *Macromolecules*, 2011, **44**, 8990–8998.
62 H. Dong, J. F. Snyder, K. S. Williams and J. W. Andzelm, *Biomacromolecules*, 2013, **14**, 3338–3345.
63 L. Mendoza, W. Batchelor, R. F. Tabor and G. Garnier, *J. Colloid Interface Sci.*, 2018, **509**, 39–46.
64 L. Lewis, M. Derakhshandeh, S. G. Hatzikiriakos, W. Y. Hamad and M. J. MacLachlan, *Biomacromolecules*, 2016, **17**, 2747–2754.
65 A. E. Way, L. Hsu, K. Shanmuganathan, C. Weder and S. J. Rowan, *ACS Macro Lett.*, 2012, **1**, 1001–1006.
66 K. J. De France, T. Hoare and E. D. Cranston, *Chem. Mater.*, 2017, **29**, 4609–4631.
67 J. R. McKee, E. A. Appel, J. Seitsonen, E. Kontturi, O. A. Scherman and O. Ikkala, *Adv. Funct. Mater.*, 2014, **24**, 2706–2713.
68 X. Yang, K. Abe, S. K. Biswas and H. Yano, *Cellulose*, 2018, **25**, 6571–6580.
69 R. E. Abouzeid, R. Khiari, D. Beneventi and A. Dufresne, *Biomacromolecules*, 2018, **19**, 4442–4452.
70 M. Ahlen, G. K. Tummala and A. Mihranyan, *Int. J. Pharm.*, 2018, **536**, 73–81.
71 W. Huang, Y. Wang, Z. Huang, X. Wang, L. Chen, Y. Zhang and L. Zhang, *ACS Appl. Mater. Interfaces*, 2018, **10**, 41076–41088.
72 Q.-F. Guan, Z.-M. Han, Y. Zhu, W.-L. Xu, H.-B. Yang, Z.-C. Ling, B.-B. Yan, K.-P. Yang, C.-H. Yin, H. Wu and S.-H. Yu, *Nano Lett.*, 2021, **21**, 952–958.
73 Q.-F. Guan, Z.-M. Han, Z.-C. Ling, H.-B. Yang and S.-H. Yu, *Nano Lett.*, 2020, **20**, 5699–5704.
74 J. Tie, H. Chai, Z. Mao, L. Zhang, Y. Zhong, X. Sui and H. Xu, *Carbohydr. Polym.*, 2021, **273**, 118600.
75 X. Zhang, J. Zhao, T. Xia, Q. Li, C. Ao, Q. Wang, W. Zhang, C. Lu and Y. Deng, *Energy Storage Mater.*, 2020, **31**, 135–145.
76 T. Budtova, *Cellulose*, 2019, **26**, 81–121.
77 N. Lavoine and L. Bergström, *J. Mater. Chem. A*, 2017, **5**, 16105–16117.
78 H. Ding, S. Qiu, X. Wang, L. Song and Y. Hu, *Cellulose*, 2021, **28**, 9769–9783.
79 Z. Chen, Z. Li, P. Lan, H. Xu and N. Lin, *Carbohydr. Polym.*, 2022, **275**, 118708.
80 N. T. Cervin, E. Johansson, P. A. Larsson and L. Wagberg, *ACS Appl. Mater. Interfaces*, 2016, **8**, 11682–11689.
81 S. Y. Park, S. Goo, H. Shin, J. Kim and H. J. Youn, *Cellulose*, 2021, **28**, 10291–10304.
82 M. Qao, X. Yang, Y. Zhu, G. Guerin and S. Zhang, *Langmuir*, 2020, **36**, 6421–6428.
83 H. Liu, H. Du, T. Zheng, K. Liu, X. Ji, T. Xu, X. Zhang and C. Si, *Chem. Eng. J.*, 2021, **426**, 130817.
84 A. Zaman, F. Huang, M. Jiang, W. Wei and Z. Zhou, *Energy Built. Environ.*, 2020, **1**, 60–76.
85 X. Zhang, X. Zhao, T. Xue, F. Yang, W. Fan and T. Liu, *Chem. Eng. J.*, 2020, **385**, 123963.
86 H.-Y. Mi, X. Jing, A. L. Politowicz, E. Chen, H.-X. Huang and L.-S. Turng, *Carbon*, 2018, **132**, 199–209.
87 Y. Chen, L. Zhang, Y. Yang, B. Pang, W. Xu, G. Duan, S. Jiang and K. Zhang, *Adv. Mater.*, 2021, **33**, e2005569.
88 F. Ram, B. Biswas, A. Torris, G. Kumaraswamy and K. Shanmuganathan, *Cellulose*, 2021, **28**, 6323–6337.
89 X. Wang, Y. Zhang, H. Jiang, Y. Song, Z. Zhou and H. Zhao, *Mater. Lett.*, 2016, **183**, 179–182.
90 C. Darpentigny, G. Nonglaton, J. Bras and B. Jean, *Carbohydr. Polym.*, 2020, **229**, 115560.
91 F. Jiang and Y. L. Hsieh, *ACS Appl. Mater. Interfaces*, 2017, **9**, 2825–2834.
92 I. Sarbu and C. Sebarchievici, *Sustainability*, 2018, **10**, 191.
93 S. Kuravi, J. Trahan, D. Y. Goswami, M. M. Rahman and E. K. Stefanakos, *Prog. Energy Combust. Sci.*, 2013, **39**, 285–319.
94 A. Sharma, V. V. Tyagi, C. R. Chen and D. Buddhi, *Renewable Sustainable Energy Rev.*, 2009, **13**, 318–345.
95 N. Nallusamy, S. Sampath and R. Velraj, *Renewable Energy*, 2007, **32**, 1206–1227.
96 J. Xu, R. Wang and Y. Li, *Sol. Energy*, 2014, **103**, 610–638.
97 G. Krese, R. Koželj, V. Butala and U. Stritih, *Energy Build.*, 2018, **164**, 239–253.
98 P. K. Singh Rathore, S. K. Shukla and N. K. Gupta, *Sustain. Cities Soc.*, 2020, **53**, 101884.
99 I. Dincer, *Energy Build.*, 2002, **34**, 377–388.
100 A. Fallahi, G. Guldentops, M. Tao, S. Granados-Focil and S. Van Dessel, *Appl. Therm. Eng.*, 2017, **127**, 1427–1441.
101 N. Zhang, Y. Yuan, X. Cao, Y. Du, Z. Zhang and Y. Gui, *Adv. Eng. Mater.*, 2018, **20**, 1700753.
102 Y. Yuan, N. Zhang, W. Tao, X. Cao and Y. He, *Renewable Sustainable Energy Rev.*, 2014, **29**, 482–498.
103 A. Abhat, *Sol. Energy*, 1983, **30**, 313–332.
104 H. Ö. Paksoy, *Thermal energy storage for sustainable energy consumption: fundamentals, case studies and design*, Springer, Dordrecht, The Netherlands, 2007.
105 V. Kapsalis and D. Karamanis, *Appl. Therm. Eng.*, 2016, **99**, 1212–1224.
106 L. Kancane, R. Vanaga and A. Blumberga, *Energy Procedia*, 2016, **95**, 175–180.
107 N. Xie, Z. Huang, Z. Luo, X. Gao, Y. Fang and Z. Zhang, *Appl. Sci.*, 2017, **7**, 1317.
108 R. Pandey, P. Thapa, V. Kumar, Y. Zhu, N. Wang, M. Bystrzejewski and S. K. Tiwari, *Materialia*, 2022, **21**, 101357.
109 T. R. Whiffen and S. B. Riffat, *Int. J. Low Carbon Technol.*, 2012, **8**, 147–158.
110 A. Sharma, R. Chauhan, M. Ali Kallioğlu, V. Chinnasamy and T. Singh, *Mater. Today: Proc.*, 2021, **44**, 4357–4363.
111 T. Kousksou, A. Jamil, T. El Rhafiki and Y. Zeraouli, *Sol. Energy Mater. Sol. Cells*, 2010, **94**, 2158–2165.
112 N. Sarier and E. Onder, *Thermochim. Acta*, 2012, **540**, 7–60.
113 M. M. Farid, A. M. Khudhair, S. A. K. Razack and S. Al-Hallaj, *Energy Convers. Manage.*, 2004, **45**, 1597–1615.
114 A. B. Rezaie and M. Montazer, *Appl. Energy*, 2020, **262**, 114501.
115 L. Cao, Y. Tang and G. Fang, *Energy*, 2015, **80**, 98–103.
116 S. I. Golestaneh, A. Mosallanejad, G. Karimi, M. Khorram and M. Khashi, *Appl. Energy*, 2016, **182**, 409–417.
117 M. M. Kenisarin, *Sol. Energy*, 2014, **107**, 553–575.

118 S. Sundararajan, A. B. Samui and P. S. Kulkarni, *J. Mater. Chem. A*, 2017, **5**, 18379–18396.
119 R. Parameshwaran, R. Jayavel and S. Kalaiselvam, *J. Therm. Anal. Calorim.*, 2013, **114**, 845–858.
120 I. M. Rasta, I. N. G. Wardana, N. Hamidi and M. N. Sasongko, *J. Thermodyn.*, 2016, **2016**, 1–8.
121 N. Soodoo, K. D. Poopalam, L. Bouzidi and S. S. Narine, *Sol. Energy Mater. Sol. Cells*, 2022, **238**, 111650.
122 W. Su, J. Darkwa and G. Kokogiannakis, *Renewable Sustainable Energy Rev.*, 2015, **48**, 373–391.
123 S. A. A. Ghani, S. S. Jamari and S. Z. Abidin, *Chem. Eng. Commun.*, 2020, **208**, 687–707.
124 X. Bao, H. Yang, X. Xu, T. Xu, H. Cui, W. Tang, G. Sang and W. H. Fung, *Sol. Energy Mater. Sol. Cells*, 2020, **208**, 110420.
125 M. Mehrali, J. E. ten Elshof, M. Shahi and A. Mahmoudi, *Chem. Eng. J.*, 2021, **405**, 126624.
126 C. Lin, S. Xu, G. Chang and J. Liu, *J. Power Sources*, 2015, **275**, 742–749.
127 S. Park, S. Woo, J. Shon and K. Lee, *Energy*, 2017, **119**, 1108–1118.
128 C. Shen, X. Li, G. Yang, Y. Wang, L. Zhao, Z. Mao, B. Wang, X. Feng and X. Sui, *Chem. Eng. J.*, 2020, **385**, 123958.
129 M. O. Jusu, G. Glauser, J. F. Seward, M. Bawoh, J. Tempel, M. Friend, D. Littlefield, M. Lahai, H. M. Jalloh, A. B. Sesay, A. F. Caulker, M. Samai, V. Thomas, N. Farrell and M. A. Widdowson, *J. Infect. Dis.*, 2018, **217**, S48–S55.
130 K. Sun, H. Dong, Y. Kou, H. Yang, H. Liu, Y. Li and Q. Shi, *Chem. Eng. J.*, 2021, **419**, 129637.
131 W. Aftab, M. Khurram, S. Jinming, H. Tabassum, Z. Liang, A. Usman, W. Guo, X. Huang, W. Wu, R. Yao, Q. Yan and R. Zou, *Energy Storage Mater.*, 2020, **32**, 199–207.
132 F. Xiong, K. Yuan, W. Aftab, H. Jiang, J. Shi, Z. Liang, S. Gao, R. Zhong, H. Wang and R. Zou, *ACS Appl. Mater. Interfaces*, 2021, **13**, 1377–1385.
133 Y. Huang, Q. Lin, H. Liu, M. Ni and X. Zhang, *Int. J. Heat Mass Transfer*, 2017, **115**, 1166–1173.
134 W. Aftab, A. Usman, J. Shi, K. Yuan, M. Qin and R. Zou, *Energy Environ. Sci.*, 2021, **14**, 4268–4291.
135 S. Gong, X. Li, M. Sheng, S. Liu, Y. Zheng, H. Wu, X. Lu and J. Qu, *ACS Appl. Mater. Interfaces*, 2021, **13**, 47174–47184.
136 O. M. Balci, M. A. Ezan and K. Z. Turhan, *Energy Storage*, 2019, **1**, e81.
137 V. S. K. V. Harish and A. Kumar, *Renewable Sustainable Energy Rev.*, 2016, **56**, 1272–1292.
138 H. Schmit, W. Pfeffer, C. Rathgeber and S. Hiebler, *Thermochim. Acta*, 2016, **635**, 26–33.
139 V. V. Tyagi and D. Buddhi, *Sol. Energy Mater. Sol. Cells*, 2008, **92**, 891–899.
140 M. Koschenz and B. Lehmann, *Energy Build.*, 2004, **36**, 567–578.
141 V. Madadi Avargani, B. Norton, A. Rahimi and H. Karimi, *Sustain. Energy Technol. Assess.*, 2021, **47**, 101350.
142 W. Wu, J. Liu, M. Liu, Z. Rao, H. Deng, Q. Wang, X. Qi and S. Wang, *Energy Convers. Manage.*, 2020, **221**, 113145.
143 Y. Wang, Z. Wang, H. Min, H. Li and Q. Li, *J. Energy Storage*, 2021, **35**, 102279.
144 R. Jilte, A. Afzal and S. Panchal, *Energy*, 2021, **219**, 119564.
145 M. Wang, Y. Wang, C. Zhang and F. Yu, *J. Energy Storage*, 2022, **45**, 103771.
146 P. S. Bhatkhande, *Master of Science*, Eastern Michigan University, 2011.
147 K. Yang, M. Venkataraman, X. Zhang, J. Wiener, G. Zhu, J. Yao and J. Militky, *J. Mater. Sci.*, 2022, **57**, 798–847.
148 K. Ma, X. Zhang, J. Ji, L. Han, X. Ding and W. Xie, *Biomater. Sci.*, 2021, **9**, 5762–5780.
149 C. Zhang, W. Lin, Q. Zhang, Z. Zhang, X. Fang and X. Zhang, *Int. J. Therm. Sci.*, 2019, **142**, 156–162.
150 A. Kuru and S. A. Aksoy, *Text. Res. J.*, 2013, **84**, 337–346.
151 M. Jiang, X. Song, G. Ye and J. Xu, *Compos. Sci. Technol.*, 2008, **68**, 2231–2237.
152 R. Ji, Q. Zhang, F. Zhou, F. Xu, X. Wang, C. Huang, Y. Zhu, H. Zhang, L. Sun, Y. Xia, X. Lin, H. Peng, Y. Zou and H. Chu, *J. Energy Storage*, 2021, **40**, 102687.
153 W. Hua, X. Zhang, M. J. Muthoka and X. Han, *Materials*, 2018, **11**, 1016.
154 W. Kong, M. Dannemand, J. Brinkø Berg, J. Fan, G. Englmair, J. Dragsted and S. Furbo, *Appl. Therm. Eng.*, 2019, **148**, 796–805.
155 J. Liu, C. Zhu, W. Liang, Y. Li, H. Bai, Q. Guo and C. Wang, *Sol. Energy*, 2019, **193**, 413–421.
156 Y. Wang, K. Yu and X. Ling, *Energy Convers. Manage.*, 2019, **198**, 111796.
157 K. Oh, S. Kwon, W. Xu, X. Wang and M. Toivakka, *Cellulose*, 2020, **27**, 5003–5016.
158 Z. Shen, S. Kwon, H. L. Lee, M. Toivakka and K. Oh, *Sol. Energy Mater. Sol. Cells*, 2021, **225**, 111028.
159 Z. Shen, K. Oh, S. Kwon, M. Toivakka and H. L. Lee, *Int. J. Biol. Macromol.*, 2021, **174**, 402–412.
160 K. Oh, Z. Shen, S. Kwon and M. Toivakka, *Cellulose*, 2021, **28**, 6845–6856.
161 Q. Zhang, L. Zhang, W. Wu and H. Xiao, *Carbohydr. Polym.*, 2020, **229**, 115454.
162 R. Methaapanon, S. Kornbongkotmas, C. Ataboonwongse and A. Soottitantawat, *Powder Technol.*, 2020, **361**, 910–916.
163 L. Pathak, G. V. N. Trivedi, R. Parameshwaran and S. S. Deshmukh, *Mater. Today: Proc.*, 2021, **44**, 1960–1963.
164 L. Cao, F. Tang and G. Fang, *Energy Build.*, 2014, **72**, 31–37.
165 C. Y. Zhao and G. H. Zhang, *Renewable Sustainable Energy Rev.*, 2011, **15**, 3813–3832.
166 G. Alva, Y. Lin, L. Liu and G. Fang, *Energy Build.*, 2017, **144**, 276–294.
167 L. Bai, W. Xiang, S. Huan and O. J. Rojas, *Biomacromolecules*, 2018, **19**, 1674–1685.
168 S. Han, S. Lyu, Z. Chen, S. Wang and F. Fu, *J. Mater. Sci.*, 2019, **54**, 7383–7396.
169 S. Han, S. Lyu, Z. Chen, F. Fu and S. Wang, *Carbohydr. Polym.*, 2020, **234**, 115923.
170 S. Huan, S. Yokota, L. Bai, M. Ago, M. Borghei, T. Kondo and O. J. Rojas, *Biomacromolecules*, 2017, **18**, 4393–4404.
171 Y. Yoo, C. Martinez and J. P. Youngblood, *Langmuir*, 2017, **33**, 1521–1532.
172 Y. Yoo, C. Martinez and J. P. Youngblood, *ACS Appl. Mater. Interfaces*, 2017, **9**, 31763–31776.

173 B. Zhang, Z. Zhang, S. Kapar, P. Ataeian, J. da Silva Bernardes, R. Berry, W. Zhao, G. Zhou and K. C. Tam, *ACS Sustainable Chem. Eng.*, 2019, **7**, 17756–17767.
174 S. Wu, P. Zhang, Z. Xu, Z. Chen and Y. Gao, *Mater. Res. Express*, 2020, **6**, 125376.
175 X. Shi, M. R. Yazdani, R. Ajdary and O. J. Rojas, *Carbohydr. Polym.*, 2021, **254**, 117279.
176 T. Winuprasith and M. Suphantharika, *Food Hydrocolloids*, 2013, **32**, 383–394.
177 I. Kalashnikova, H. Bizot, B. Cathala and I. Capron, *Biomacromolecules*, 2012, **13**, 267–275.
178 J. Mengjin, S. Xiaoqing, X. Jianjun and Y. Guangdou, *Sol. Energy Mater. Sol. Cells*, 2008, **92**, 1657–1660.
179 C. E. F. Tyrone and L. Vigo, *Text. Res. J.*, 1982, **52**, 633–637.
180 S. Salimian, M. Montazer, A. S. Rashidi, N. Soleimani and A. Bashiri Rezaie, *J. Appl. Polym. Sci.*, 2021, **138**, e51357.
181 S. Alay, F. Göde and C. Alkan, *Fibers Polym.*, 2010, **11**, 1089–1093.
182 C. Chen, L. Wang and Y. Huang, *Polymer*, 2007, **48**, 5202–5207.
183 H. You-Lo, in *Advanced Green Composites*, ed. A. Netravali, Scrivener Publishing LLC, Beverly, MA, U. S. A., 2014, ch. 4, pp. 67–96.
184 Y. Wang, X. Wang, Y. Xie and K. Zhang, *Cellulose*, 2018, **25**, 3703–3731.
185 M. Qu, C. Guo, L. Li and X. Zhang, *J. Therm. Anal. Calorim.*, 2017, **130**, 781–790.
186 Ö. Gök, C. Alkan and Y. Konuklu, *Sol. Energy Mater. Sol. Cells*, 2019, **191**, 345–349.
187 S. Y. H. Abdalkarim, H. Yu, C. Wang, Y. Chen, Z. Zou, L. Han, J. Yao and K. C. Tam, *Chem. Eng. J.*, 2019, **375**, 121979.
188 S. Y. H. Abdalkarim, Z. Ouyang, H. Y. Yu, Y. Li, C. Wang, R. A. M. Asad, Y. Lu and J. Yao, *Carbohydr. Polym.*, 2021, **254**, 117481.
189 S. Y. H. Abdalkarim, H.-Y. Yu, D. Wang and J. Yao, *Cellulose*, 2017, **24**, 2925–2938.
190 S. Y. H. Abdalkarim, H.-Y. Yu, C. Wang, L. Yang, Y. Guan, L. Huang and J. Yao, *ACS Appl. Bio Mater.*, 2018, **1**, 714–727.
191 J. Shi, W. Aftab, Z. Liang, K. Yuan, M. Maqbool, H. Jiang, F. Xiong, M. Qin, S. Gao and R. Zou, *J. Mater. Chem. A*, 2020, **8**, 20133–20140.
192 Y. Cai, X. Song, M. Liu, F. Li, M. Xie, D. Cai and Q. Wei, *J. Therm. Anal. Calorim.*, 2016, **128**, 661–673.
193 C. E. Tas, E. Berksun, D. Koken, S. Kolgesiz, S. Unal and H. Unal, *Ind. Eng. Chem. Res.*, 2021, **60**, 14788–14800.
194 Z. Shi, H. Xu, Q. Yang, C. Xiong, M. Zhao, K. Kobayashi, T. Saito and A. Isogai, *Carbohydr. Polym.*, 2019, **225**, 115215.
195 M. N. Fukuya, K. Senoo, M. Kotera, M. Yoshimoto and O. Sakata, *Biomacromolecules*, 2017, **18**, 4411–4415.
196 Y. Li, S. Yu, P. Chen, R. Rojas, A. Hajian and L. Berglund, *Nano Energy*, 2017, **34**, 541–548.
197 Y. He, H. Li, F. Luo, Y. Jin, B. Huang and Q. Qian, *Composites, Part A*, 2021, **151**, 106638.
198 Y. Wang, Z. Qiu, Z. Lang, Y. Xie, Z. Xiao, H. Wang, D. Liang, J. Li and K. Zhang, *Adv. Mater.*, 2021, **33**, e2005263.
199 C. Zhou, R. Chu, R. Wu and Q. Wu, *Biomacromolecules*, 2011, **12**, 2617–2625.
200 J.-C. Liu, D. J. Martin, R. J. Moon and J. P. Youngblood, *J. Appl. Polym. Sci.*, 2015, **132**, 41970.
201 S. Malmir, B. Montero, M. Rico, L. Barral and R. Bouza, *Composites, Part A*, 2017, **93**, 41–48.
202 X. Du, J. Qiu, S. Deng, Z. Du, X. Cheng and H. Wang, *ACS Appl. Mater. Interfaces*, 2020, **12**, 5695–5703.
203 Z. Shen, S. Kwon, H. L. Lee, M. Toivakka and K. Oh, *Carbohydr. Polym.*, 2021, **273**, 118585.
204 Y. Li, Y. Chen, X. Huang, S. Jiang and G. Wang, *Chem. Eng. J.*, 2021, **415**, 129086.
205 B. Bari, J. Lee, T. Jang, P. Won, S. H. Ko, K. Alamgir, M. Arshad and L. J. Guo, *J. Mater. Chem. A*, 2016, **4**, 11365–11371.
206 F. Xue, X. Z. Jin, W. Y. Wang, X. D. Qi, J. H. Yang and Y. Wang, *Nanoscale*, 2020, **12**, 4005–4017.
207 J. Xu, Y. Tan, X. Du, Z. Du, X. Cheng and H. Wang, *Cellulose*, 2020, **27**, 9547–9558.
208 J. Chen, Y. Zhang, F. Wu, B. Guan, X. Du and H. Wang, *Cellulose*, 2021, **28**, 9739–9750.
209 X. Du, M. Zhou, S. Deng, Z. Du, X. Cheng and H. Wang, *Cellulose*, 2020, **27**, 4679–4690.
210 X. Wei, X. Z. Jin, N. Zhang, X. D. Qi, J. H. Yang, Z. W. Zhou and Y. Wang, *Carbohydr. Polym.*, 2021, **253**, 117290.